THERMAL ANALYSIS OF WIRE-SCREEN REGENERATOR MATRIX USING CFD

A THESIS SUBMITTED IN PARTIAL FULFILLMENT OF THE REQUIREMENTS FOR THE DEGREE OF

Bachelor of Technology

In

Mechanical Engineering

By

SIDHARTH PRADHAN

AND

SUSHEEL KUMAR SINGH

Under the Guidance of

PROF. SUNIL KUMAR SARANGI

Department of Mechanical Engineering

National Institute of Technology

Rourkela

National Institute of Technology

Rourkela

CERTIFICATE

This is to certify that the thesis entitled "**THERMAL ANALYSIS OF WIRE-SCREEN REGENERATOR MATRIX USING CFD"** submitted by **SIDHARTH PRADHAN** and **SUSHEEL KUMAR SINGH** in partial fulfilment of the requirements for the award of Bachelor of technology Degree in Mechanical Engineering at the National Institute of Technology, Rourkela (Deemed University) is an authentic work carried out by him under my supervision and guidance.

To the best of my knowledge, the matter embodied in the thesis has not been submitted to any other University / Institute for the award of any Degree or Diploma.

Prof. Sunil Kumar Sarangi

Date: National Institute of Technology

Rourkela

ACKNOWLEDGEMENT

We would like to express my deep sense of gratitude and respect to our mentor and guide Prof. Sunil Kumar Sarangi, for his excellent guidance and suggestions. He has been a motivating factor for us. We feel extremely lucky to get a chance to work under the guidance of such a dynamic personality.

We am also highly indebted to Prof. Ramjee Repeka and Prof. K.P. Maity for their constant motivation and support.

Last but not the least; we would also like to thank Ejaz sir and Rahul Goyal for their in-depth understanding and unrelenting cooperation.

Sidharth Pradhan
Roll No- 10603
8th Semester B.Tech.
Department of Mechanical Engineering

Susheel Kumar Singh
Roll No-10603049
8th Semester B.Tech.
Department of Mechanical Engineering

TABLE OF CONTENTS

LIST OF TABLES

LIST OF FIGURES

TABLE OF GRAPHS

SINGLE WIRE ANALYSIS

Nu Vs angle

FOUR WIRE ANALYSIS

Nu Vs angle(Front)

Nu Vs angle(back)

ABSTRACT

Wire screen meshes or screen matrix have been widely used in aviation, chemical reaction, refrigeration, food processing, heat dissipation, aerospace, electronics, combustion, cryogenics and other applications. These are used as heat exchanger material due to higher surface area density resulting in higher heat dissipation. The CFD code used to study the fluid flow over wire screen is FLUENT. The initial study has been limited to 2-D analysis of flow over wires in one wire, four wires and nine wires in an inline arrangement. The angle of minimum Nusselt number has been plotted against Reynolds number for same geometry to find a correlation for low Re (0.015-15) and to better understand the flow over wires, Nusselt number has also been plotted w.r.t. circumferential angle. The analysis has been further extended to 3D analysis of 200 and 400 wire screen meshes to observe the change in pressure drop with Re.

Keywords: Porosity, Reynolds number, Nusselt number, surface heat transfer coefficient

CHAPTER 1

INTRODUCTION

Cryocoolers are used for maintaining low temperature which is quite necessary for various applications like liquefaction of gases, separation of gases, study of superconductivity, cryomachining, cryosurgery etc. Gas separation is necessary for various reasons like welding (TIG, MIG and PAW), manufacture of fertilizers, rocket propulsion, nuclear energy etc.

There are two types of Cryocoolers on the basis of heat exchangers used. They are:-

1. Recuperative type
2. Regenerative type

In recuperative heat exchangers, heat is exchanged by flow of fluid at different temperature across two sides of a dividing wall. Regenerative heat exchangers act as thermal flywheels, storing excess heat in one part of the cycle and releasing it in the next. The efficiency of regenerative Cryocoolers like Gifford-McMohan, stirling and pulse tube refrigerators depends to a large extent on the performance of the regenerator matrix.

Regenerator is made up of wire mesh screens stacked one over the other. The fine wire mesh is commonly obtained in the form of woven screen at variety of wire sizes, weave structures, mesh density, porosity and material used. Other types of regenerator matrices are also used such as spheres made of stainless steel, bronze, lead and erbium. These wire meshes used are manufactured in standard sizes like 100 mesh, 200 mesh,400 mesh etc. A 400 wire mesh screen means that there would be 400 X 400 pores per sq. Inch.

Wire mesh is a large regulatory category of wire fabric. It is made out of chemical fibres, silk, metal wire through certain weaving methods Wire – screen meshes or Screen matrix have been widely used in Aviation, chemical reaction, refrigeration, food processing, heat dissipation, aerospace, printing, dyeing, electronics, combustion and other application. Up to the most advanced technology, down to daily life and culture, wire mesh screen develops simultaneously with the national economy and plays an important role in the peoples' daily life. These structures are more effective in dissipating heat due to large values of surface area density.

CHAPTER 2

HISTORY REVIEW

Recently many studied has been going on over the wire screen matrix, with the development of small crycooler now a days, gradually the researchers are concentrated on increasing the performance of small size regenerator. Thus adopting different arrangement for wire screen, variety of wire sizes, weave structures, mesh material and density. Uri & Manitakos [2] designed ,analyzed, fabricated and tested a laminate screen matrix regenerator with 47 elements. The laminate was fabricated from stainless steel screen sheets that were stacked on top of each other at certain angular orientation and then bonded at high temperature and pressure environment utilizing a sintering process. Regenerator cost and performance comparison data between the conventional widely used method of stacked screens and the new stacked laminate matrix regenerator was discussed. Armour and cannon [5], Ergun [4], experimentally investigated the flow through the wire screen structures and determination of frictional factors was discussed. Tian et al. [7] measured both the pressure loss and heat transfer performance characteristics of brazed mesh structures in forced air convection . Robinson and Richards [6] studied the effect of wire shapes on pressure drop and found that the friction factor depends both on structure porosities and the diameter of wires and concept of effective porosity has been proposed. It was found that for a fixed surface area density there exists an optimal porosity (0.8) for maximal heat dissipation. Kolb et al. found that the wire screen matrix yields an improved thermal performance with higher heat transfer rates and smaller friction losses compared to traditional flat-plate design. They also suggested that a simulation model is needed for design optimisation because of the large number of design and operation parameters.

To simulate fluid flow and heat transfer across wire-screen meshes, researchers treated these structures as porous media. Hsu et al. Studied the thermal conductivity of wire screens at the stagnant situation by considering only the conduction of wire-screen layers saturated with fluid. Wirtz and co-workers also used a conduction model to calculate the effective conductivity :

their predictions agree with experimental measurement for airflow, as the fluid conductivity is insignificant.

Chang established the correlation between effective thermal conductivity and structure porosity. Xu et al [1] establishes a direct numerical simulation on the fluid flow and heat transfer characteristics at the structure pore level. The geometry domain for complex mesh screen is reasonably simplified for an affordable numerical model.

In the present study, 1wire,4 wire ,9 wire analysis was done gradually increasing the disturbances from the surrounding. It helps us to understand the flow around the wires and very helpful for obtaining correlation between different flow conditions. Then wire mesh screen analysis was done shifting from 2D to 3D geometry, taking 400 meshes and thus obtained pressure drop through regenerator of certain length.

CHAPTER 3

THEORY

Regenerators are an essential part of a cryocooler. It performs the function of a temporary energy storage device and facilitates in the operation of a cycle at higher energy efficiency.

The data used in the analysis considers flow of helium in a stirling cycle refrigerator. The regenerator matrix material is taken as steel.

Regenerator used in Stirling cycle

Stirling cycle consists of two isothermal processes and two isochoric processes. It can be demonstrated by either alpha type (double cylinder) or beta type (single cylinder). Alpha type may have an opposed piston or V-type cylinder configuration.

Considering an opposed piston configuration with a regenerator separating the two chambers, one of the two swept volumes is called the expansion space and is kept at low temperature T_E. The other volume is called the compression space which is maintained at ambient temperature T_C.

It consists of 4 thermodynamic processes. They are:

1. **Isothermal compression**
   During compression, the fluid in the compression space is compressed as the piston moves towards the inner dead point and the expansion space piston remains stationary. The working fluid is compressed and pressure increases as a result. The temperature is constant because heat Q_C is abstracted from the compression space cylinder.

2. **Isochoric heat release**
   Both pistons move simultaneously, the compression piston towards and the expansion space piston away from the regenerator. There is no change in volume. The fluid

passing through the regenerator loses heat to it leading to fall in temperature to T_E. The decrease in temperature is accompanied by a fall in pressure.

3. **Isothermal expansion**

   The expansion piston moves to the outer dead point, while the compression piston remains stationary. The fluid absorbs heat Q_E from the surroundings and expands causing the cooling or refrigeration. The temperature remains constant and pressure falls.

4. **Isochoric heat absorption**

   Both pistons move simultaneously so that the working fluid is passed through the regenerator from the expansion space to the compression space. The matrix heats the passing fluid causing it to emerge at T_C from the matrix.

For inline cylinder arrangement, Re is calculated as:

$Re= \rho U_\infty D_h/\mu$

$D_h = D*(P/P-D)$

To calculate porosity of mesh screen:

Mesh screen = 400x400 (400mesh in 1inch),

t (screen thickness)=2D, L=1m

Diameter of wire =$2x10^{-5}$m

Fig. 1 Wire screen

Volume of one wire=$3.14/4*D^2*L$

Total no. of wire = 15748+15748 = 31496

Total wire volume= $(31,496)*3.14*10^{-10}$

Total screen volume= $L*L*t=4x10^{-5}$ m^3

Void volume = Total screen volume-Total wire volume

$=3.01103 \text{ X } 10^{-5}$

Porosity (β) = Void volume/ Total screen volume = 0.75

For wire screen mesh, Re is calculated as:

$$Re= \rho U_{\infty} D_h/\mu$$

$$;D_h=(\beta/1-\beta)*D$$

3.2 **WHAT IS CFD?**

Computational fluid dynamics is the analysis of systems involving fluid flow, heat transfer and associated phenomena such as chemical reactions by means of computer based simulation. The technique is very powerful and spans a wide range of industrial application areas. Some examples are:

- Aerodynamics of aircraft and vehicles: lift and drag
- Hydrodynamics of ships
- Power plant: combustion in IC engines and gas turbines
- Turbo machinery: fluid inside rotating passages, diffusers etc.
- Electrical and electronic engineering : cooling of equipment including micro circuits
- Chemical process engineering : mixing and separation ,polymer moulding
- External and internal environment of buildings : wind loading and heating/ventilation
- Marine engineering : loads on off –shore structures
- Environmental engineering :distribution of pollutants and effluents
- Hydrology and oceanography : flows in rivers ,estuaries, oceans
- Meteorology: Weather prediction
- Biomedical engineering : blood flows through arteries and veins

The ultimate aim of developments in the CFD field is to provide a capability comparable to other CAE (computer –aided Engineering) tools such stress analysis codes .Moreover, there are several unique advantages of CFD over experiment-based approaches to fluid systems design:

- Substantial reduction of lead times and costs of new designs
- Ability to study systems where controlled experiment are difficult or impossible to perform
- Ability to study systems under hazardous conditions at and beyond their normal performance limits
- Practically unlimited level of detail of results

The variable cost of an experiment ,in terms of facility hire and/or man-hour costs , is proportional to the number of data points and the number of configuration tested .In contrast CFD codes can produce extremely large volumes of results at virtually no added expense and it is very cheap to perform parametric studies ,for instance to optimise equipment performance.

3.3 How does a CFD code work?

CFD codes are structured around the numerical algorithms that can tackle fluid flow problems .In order to provide easy access to their interfaces to input problem parameters and to examine the results. Hence all codes contain three main elements:

- A pre-processor
- A solver
- A post-processor

Pre-processor

Pre-processing consists of the input of a flow problem to a CFD program by means of an operator –friendly interface and the subsequent transformation of this input into a form suitable for use by the solver. The user activities at the pre-processing stage involve:

- Definition of the geometry of the region of interest: computational domain.
- Grid generation –the sub-division of the domain into a number of smaller , non-overlapping sub-domains: a grid(or mesh) of cells

- Selection of the physical and chemical phenomena that need to be modelled
- Definition of fluid properties
- Specification of appropriate boundary conditions at cells which coincide with or touch the domain boundary.

Solver

There are three distinct streams of numerical solution techniques: finite difference, finite element and spectral methods .In outline the numerical methods that form that basis of the solver perform the following steps:

- Approximation of the unknown flow variables by means of simple functions
- Discretisatio n by substitution of the approximations into governing flow equations and subsequent mathematical manipulations.
- Solution of the algebraic equation.

Post-Processor

A huge amount of development work has recently taken place in the post-processing field. Owing to the increased popularity of engineering workstations, many of which have outstanding graphics capabilities, the leading CFD packages are now equipped with versatile data visualisation tools. These include:

- Domain geometry and grid display
- Vector plus
- Line and shaded contour plots
- 2d and 3d surface plots
- Particle tracking
- View manipulation

3.4 Setting up problem in FLUENT

Step 1 - **Geometry creation and grid generation.**

- Triangular meshes

Step 2 - **Solver.**

- pressure based

- 2D/3D

- steady.

- implicit.

- absolute velocity formulation.

- remaining by default.

Step 3 - **Viscous model**.

-Laminar

Step 4 - **Materials.**

Fluid (Helium)- density = 0.6125kg/m^3.

Viscosity = 1.99e-5 kg/m- sec.

Conductivity = 0.152w/m-K

Specific heat = 5193J/kg-K.

Solid (steel) - density = 8030kg/m^3.

Conductivity = 16.27w/m-K

Specific heat = 502.48J/kg-K.

Step 5 - **Boundary conditions.**

Inlet - velocity inlet.

Magnitude = depends on Re

Temperature =295

Outlet - outflow.

Rest is isothermal (300k) steel wall

Step 6 - **Solution control**.

Pressure - velocity coupling - simple.

Discretization- pressure - presto.

Momentum – 1st order

Under relaxation factor (value as default)

Step 7 - **Solution initialization.**

Compute from velocity inlet.

Step 8- **Iteration**.

No. of iterations - 500.

Solution converges after 100 -200 iterations.

Governing equation:

Continuity equation

$$\frac{\partial \rho}{\partial t} + \nabla \cdot (\rho \vec{V}) = 0$$

Momentum equation:

x-component:

$$\frac{\partial}{\partial t}(\rho u) + \frac{\partial}{\partial x}(\rho u^2 + p) + \frac{\partial}{\partial y}(\rho uv) + \frac{\partial}{\partial z}(\rho uw) = \rho f_x + \frac{\partial}{\partial x}(\tau_{xx}) + \frac{\partial}{\partial y}(\tau_{xy}) + \frac{\partial}{\partial z}(\tau_{xz})$$

y-component:

$$\frac{\partial}{\partial t}(\rho v) + \frac{\partial}{\partial x}(\rho uv) + \frac{\partial}{\partial y}(\rho v^2 + p) + \frac{\partial}{\partial z}(\rho vw) = \rho f_y + \frac{\partial}{\partial x}(\tau_{xy}) + \frac{\partial}{\partial y}(\tau_{yy}) + \frac{\partial}{\partial z}(\tau_{yz})$$

z-component:

$$\frac{\partial}{\partial t}(\rho w) + \frac{\partial}{\partial x}(\rho uw) + \frac{\partial}{\partial y}(\rho vw) + \frac{\partial}{\partial z}(\rho w^2 + p) = \rho f_z + \frac{\partial}{\partial x}(\tau_{xz}) + \frac{\partial}{\partial y}(\tau_{yz}) + \frac{\partial}{\partial z}(\tau_{zz})$$

Energy equation

$$\rho \frac{de_t}{dt} = \rho(uf_x + vf_y + wf_z) + \frac{\partial}{\partial x}[-pu + u\tau_{xx} + v\tau_{xy} + w\tau_{xz} - q_x]$$
$$+ \frac{\partial}{\partial y}[-pv + u\tau_{yx} + v\tau_{yy} + w\tau_{yz} - q_y] + \frac{\partial}{\partial z}[-pw + u\tau_{zx} + v\tau_{zy} + w\tau_{zz} - q_z]$$

CHAPTER 4

SINGLE WIRE ANALYSIS

Flow over single wire was examined with very low Re (0.015-15).Grid was generated and analysis was done in FLUENT. Velocity vector, Pressure contour and Temperature contour around the wire were obtained but, it is shown here for Re=1.46

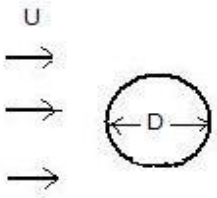

Fig 2. Real geometry

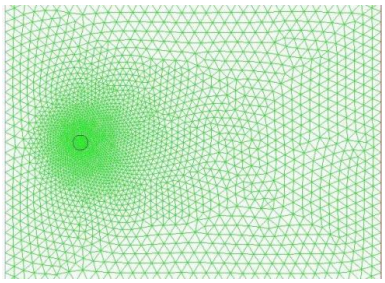

Fig 3. Mesh geometry

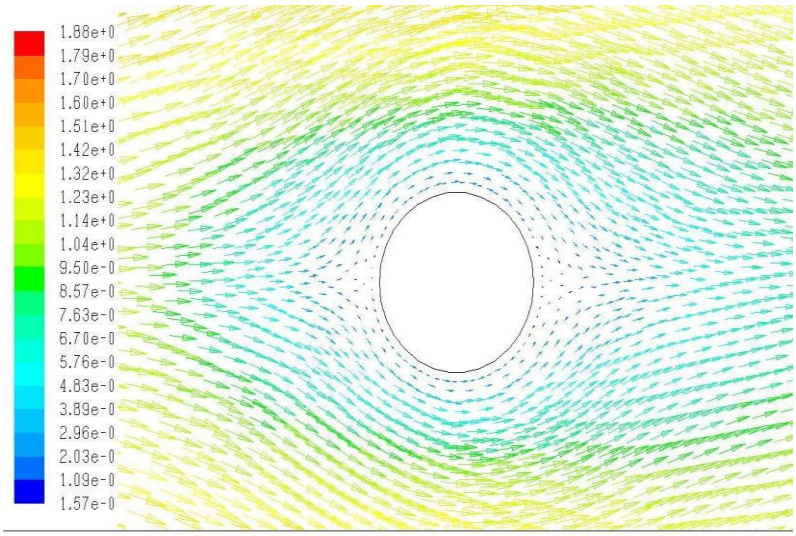

Fig.4 Velocity vector (in ms^{-1})

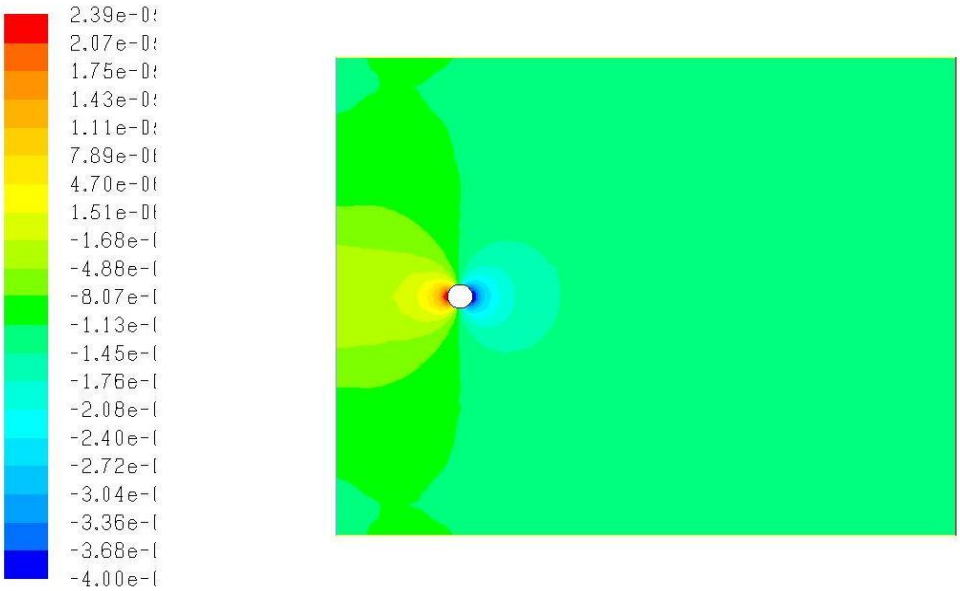

Fig 5. Pressure contour (in atm)

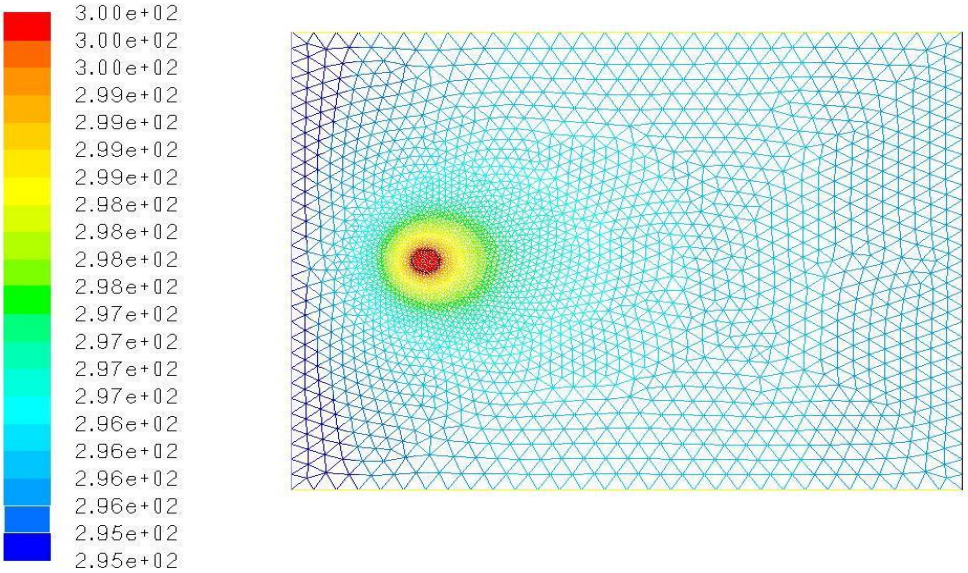

Fig 6. Temperature contour (in Kelvin)

Heat transfer coefficient was examined along circumference of wire with helium as working fluid (295 k) and steel wire (300k).Angle is taken between -180° to 180 °(with centre as origin) with anticlockwise direction w.r.t. 'X'-axis as positive and clockwise as negative. The value of Nu for various angles at Re=0.015 gave the following result. The graphs plotted showed the variation in Nu vs. Angle for different values of Re.

Surface Heat Transfer Coefficient	x	y	Angle (in deg.)	Nu
2548.35	-1.00E-05	-1.22E-21	-1.80E+02	0.336861
2544.56	-9.78E-06	-2.08E-06	-1.68E+02	0.33636
2535.44	-9.14E-06	-4.07E-06	-1.56E+02	0.335154
2523.13	-8.09E-06	-5.88E-06	-1.44E+02	0.333527
2508.24	-6.69E-06	-7.43E-06	-1.32E+02	0.331558
2489.4	-5.00E-06	-8.66E-06	-1.20E+02	0.329068
2468.61	-3.09E-06	-9.51E-06	-1.08E+02	0.32632
2448.83	-1.05E-06	-9.95E-06	-9.60E+01	0.323705
2431.52	1.05E-06	-9.95E-06	-8.40E+01	0.321417
2416.25	3.09E-06	-9.51E-06	-7.20E+01	0.319399
2403.61	5.00E-06	-8.66E-06	-6.00E+01	0.317728
2394.52	6.69E-06	-7.43E-06	-4.80E+01	0.316526
2387.46	8.09E-06	-5.88E-06	-3.60E+01	0.315593
2382.15	9.14E-06	-4.07E-06	-2.40E+01	0.314891
2377.94	9.78E-06	-2.08E-06	-1.20E+01	0.314334
2376.77	1.00E-05	0	0.00E+00	0.31418
2378.44	9.78E-06	2.08E-06	1.20E+01	0.314401
2382.38	9.14E-06	4.07E-06	2.40E+01	0.314921
2387.85	8.09E-06	5.88E-06	3.60E+01	0.315644
2394.44	6.69E-06	7.43E-06	4.80E+01	0.316516
2402.95	5.00E-06	8.66E-06	6.00E+01	0.31764
2415.02	3.09E-06	9.51E-06	7.20E+01	0.319236
2430.34	1.05E-06	9.95E-06	8.40E+01	0.321261
2448.18	-1.05E-06	9.95E-06	9.60E+01	0.323619
2467.96	-3.09E-06	9.51E-06	1.08E+02	0.326234
2486.11	-5.00E-06	8.66E-06	1.20E+02	0.328633
2506.42	-6.69E-06	7.43E-06	1.32E+02	0.331318
2524.87	-8.09E-06	5.88E-06	1.44E+02	0.333757
2536.28	-9.14E-06	4.07E-06	1.56E+02	0.335265
2544.79	-9.78E-06	2.08E-06	1.68E+02	0.33639

Table –1: Nu for various angles over a single wire at Re=0.015

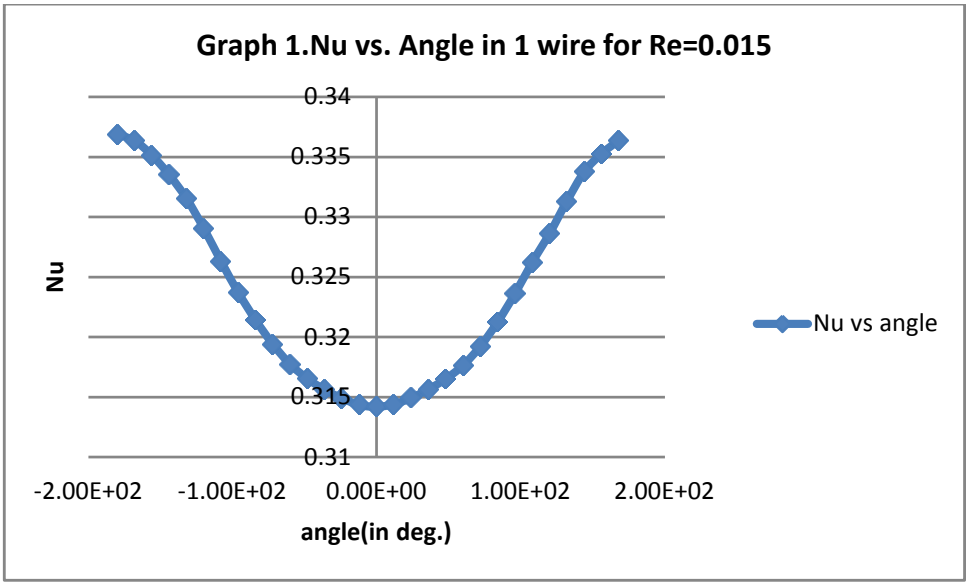
Graph 1.Nu vs. Angle in 1 wire for Re=0.015
0.34
0.335
0.33
0.325
0.32
0.315
0.31
Nu
-2.00E+02
-1.00E+02
0.00E+00
1.00E+02
2.00E+02
angle(in deg.)
Nu vs angle

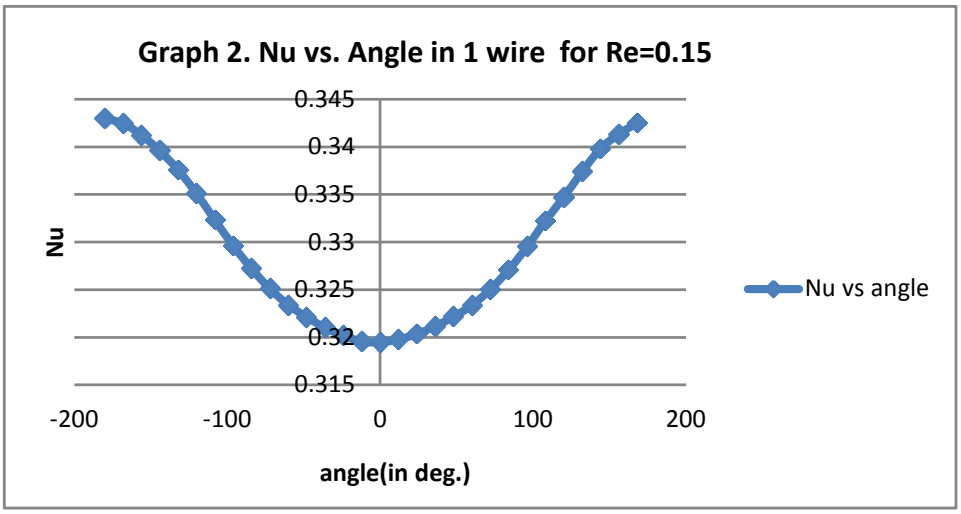
Graph 2. Nu vs. Angle in 1 wire for Re=0.15
0.345
0.34
0.335
0.33
0.325
0.32
0.315
Nu
-200
-100
0
100
200
angle(in deg.)
Nu vs angle

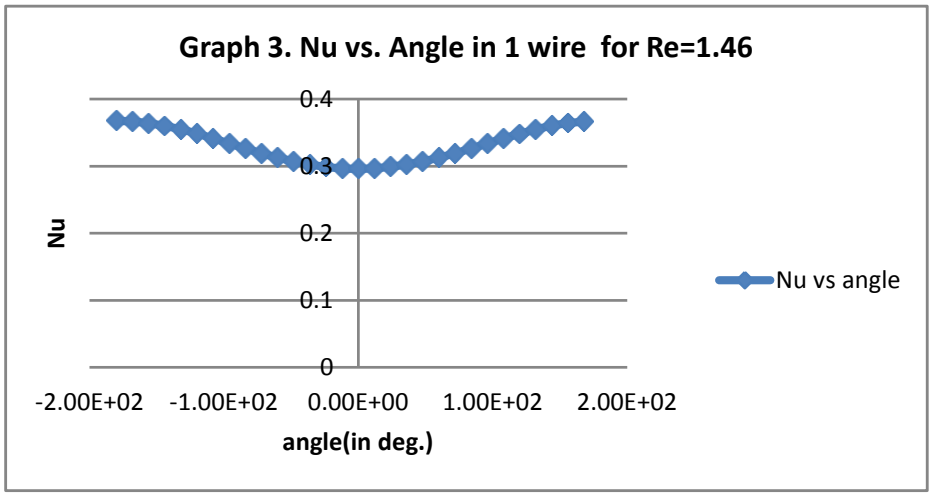
Graph 3. Nu vs. Angle in 1 wire for Re=1.46
0.4
0.3
0.2
0.1
0
Nu
-2.00E+02
-1.00E+02
0.00E+00
1.00E+02
2.00E+02
angle(in deg.)
Nu vs angle

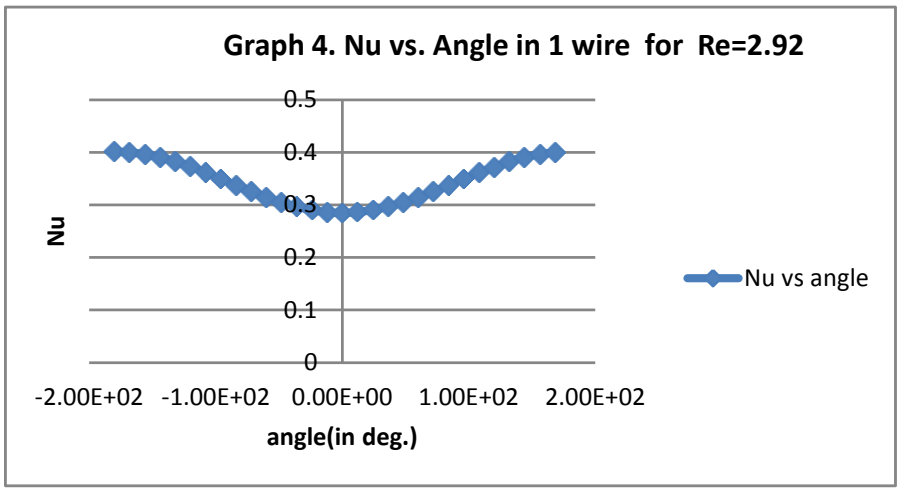
Graph 4. Nu vs. Angle in 1 wire for Re=2.92
0.5
0.4
0.3
0.2
0.1
0
Nu
-2.00E+02
-1.00E+02
0.00E+00
1.00E+02
2.00E+02
angle(in deg.)
Nu vs angle

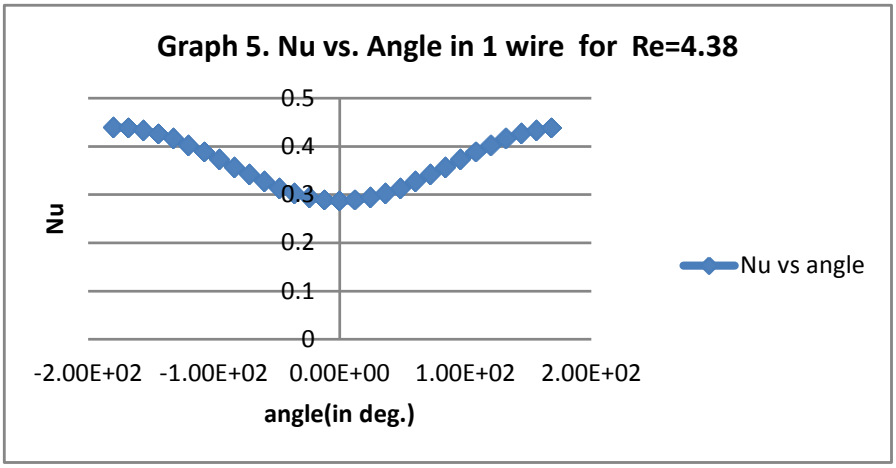
Graph 5. Nu vs. Angle in 1 wire for Re=4.38
0.5
0.4
0.3
0.2
0.1
0
Nu
-2.00E+02
-1.00E+02
0.00E+00
1.00E+02
2.00E+02
angle(in deg.)
Nu vs angle

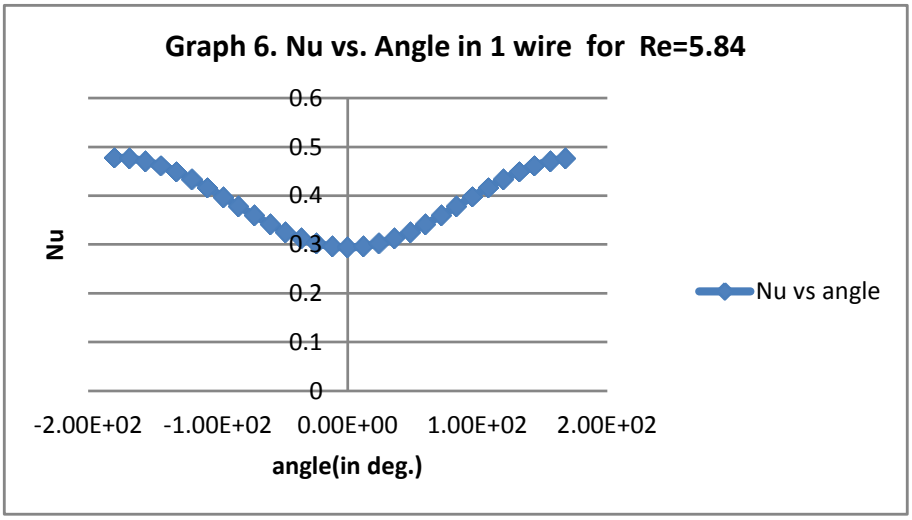
Graph 6. Nu vs. Angle in 1 wire for Re=5.84
0.6
0.5
0.4
0.3
0.2
0.1
0
Nu
-2.00E+02
-1.00E+02
0.00E+00
1.00E+02
2.00E+02
angle(in deg.)
Nu vs angle

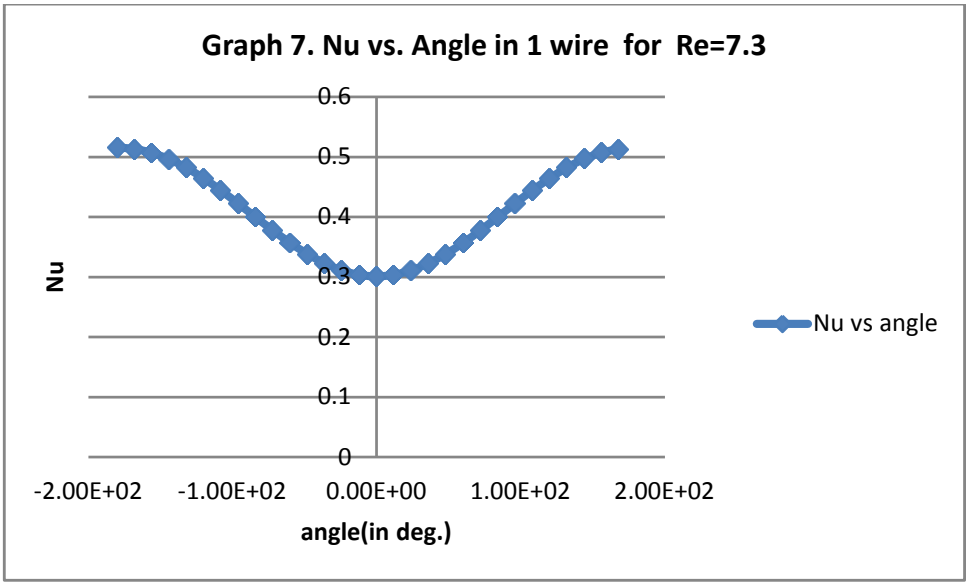

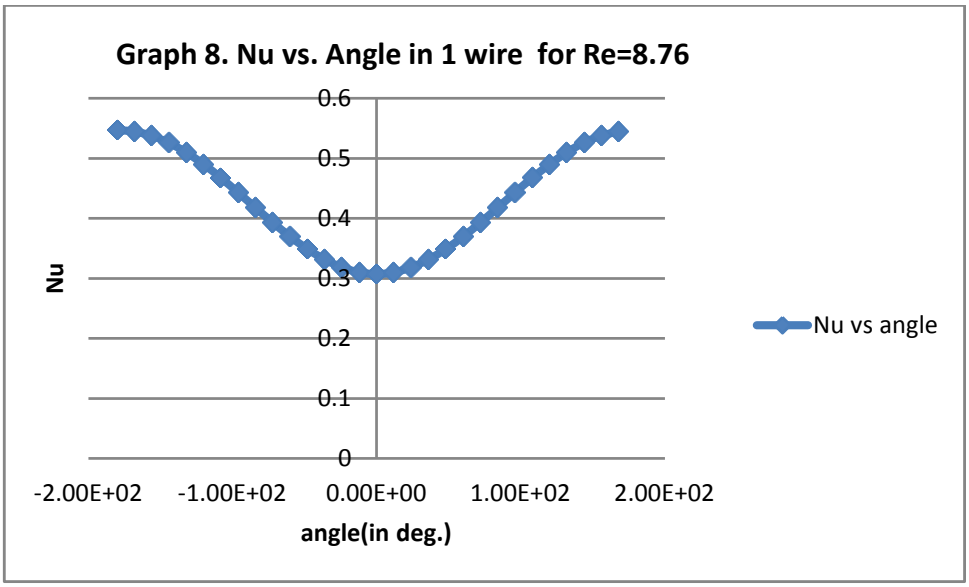

The graphs show that the variation in Nu vs. angle is high for extremely low values of Re. But the value of average Nu increases with Re. The graph becomes flat as the value of Re approaches 1. Then it again ebbs more with increase in Re.

CHAPTER 5

FOUR WIRE ANALYSES

The single wire cross flow analysis is a typical study of a bluff body without any interaction with the surrounding objects. However, the flow pattern can vary if there are other bodies near it. This variation influences the heat transfer and the Nusselt number. The point of minimum Nusselt number varies with change in Reynolds number (Re).Now, extending the analysis to four wires in an inline arrangement, the pitch (p) was taken to be $63.5X10^{-6}$ m. The diameter of the wire (D) was taken as $20X10^{-6}$ m. Grid was generated and analysis was done in FLUENT. Velocity vector, Pressure contour and Temperature contour around the wires were obtained but, it is shown here for Re=1.46

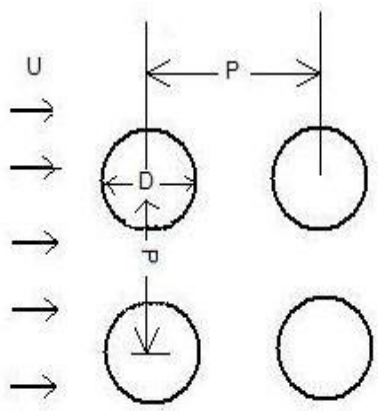

Fig 7. Real geometry

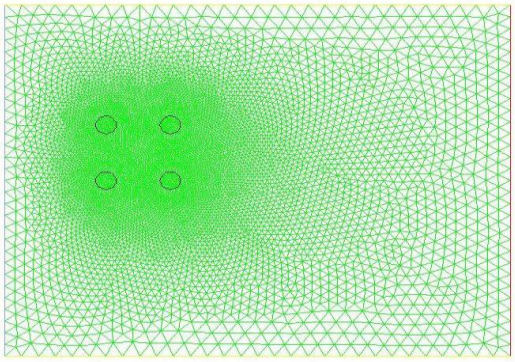

Fig 8. Mesh geometry

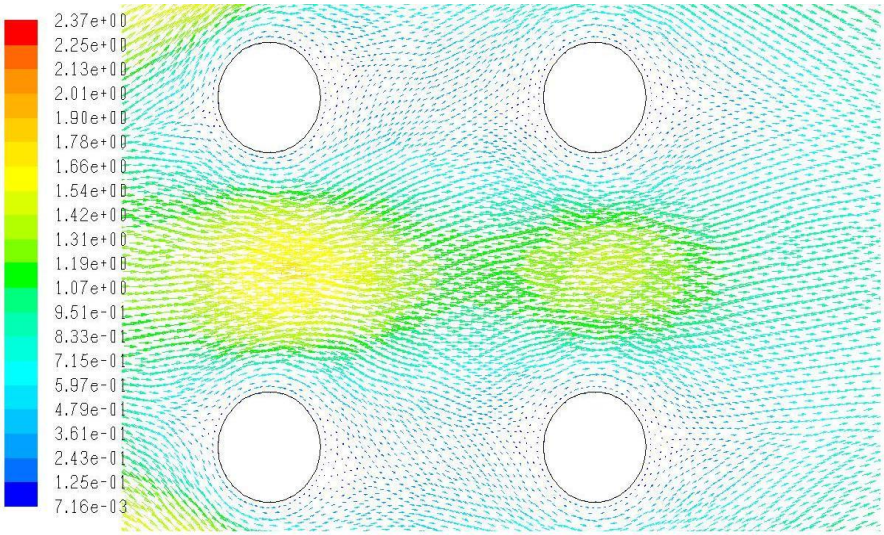

Fig 9. Velocity vector(ms^{-1})

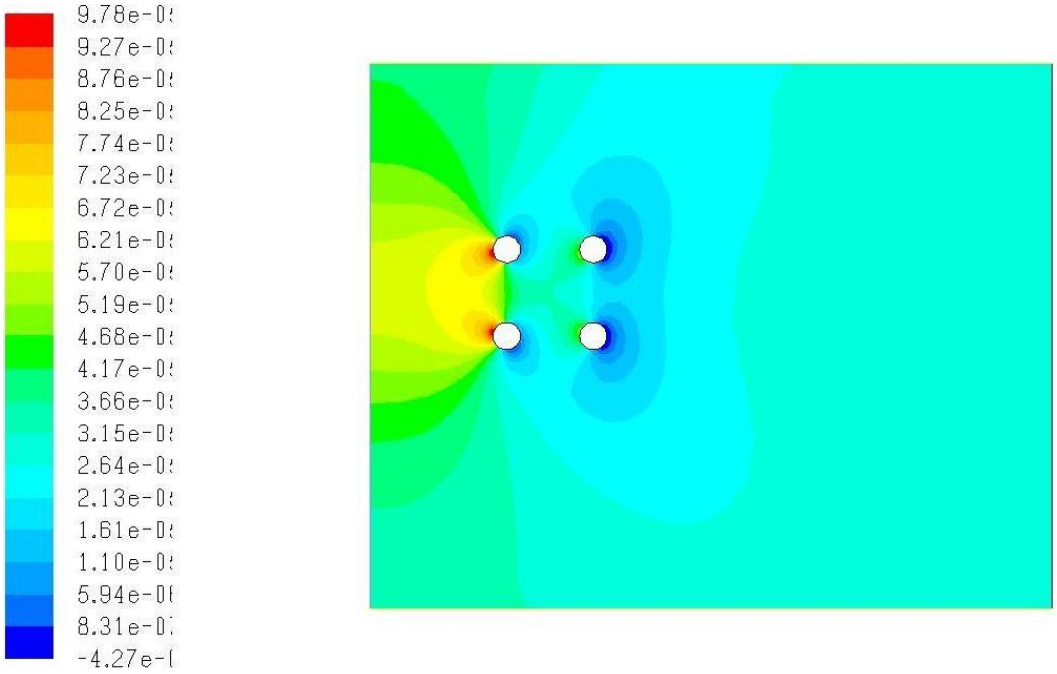

Fig.10 Pressure contour

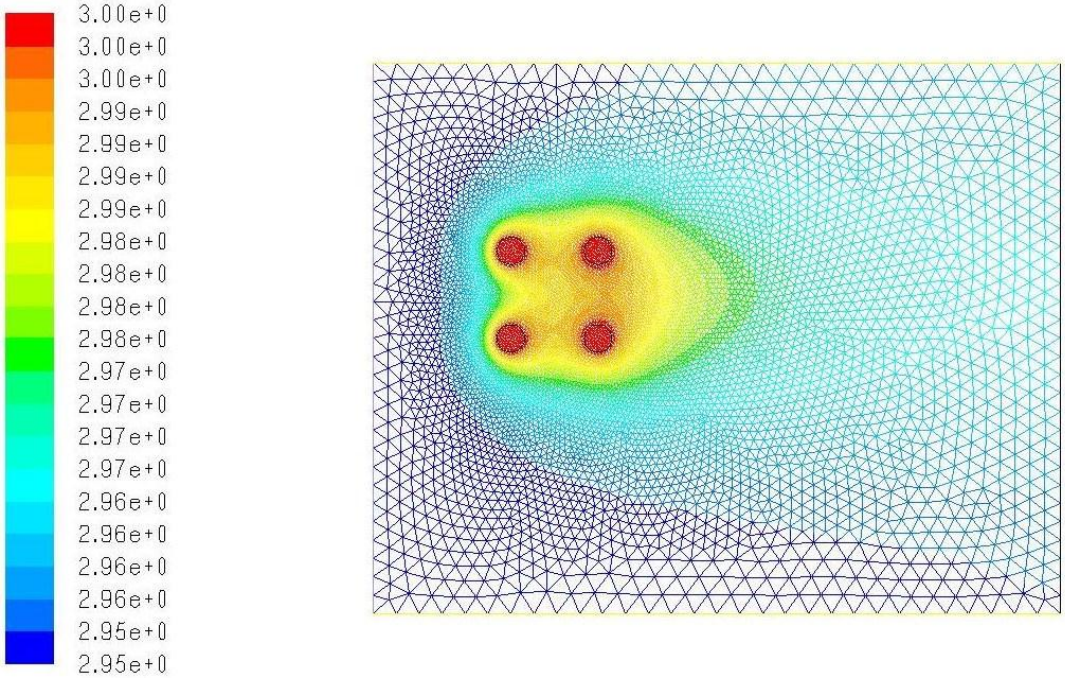

Fig 11. Temperature contour

The heat transfer coefficient was found for each point over the wire and heat transfer coefficient was used to calculate Nusselt number at a point. The table below shows Nu for various angles on the front cylinder for Re=0.015. the graphs of Nu vs. Angle for various Re was plot

Surface Heat Transfer Coef.	x	y	Angle (in deg.)	Nu
388.653	-1.00E-05	-1.22E-21	-1.80E+02	0.051375
402.589	-9.78E-06	-2.08E-06	-1.68E+02	0.053217
412.398	-9.14E-06	-4.07E-06	-1.56E+02	0.054514
418.238	-8.09E-06	-5.88E-06	-1.44E+02	0.055286
420.278	-6.69E-06	-7.43E-06	-1.32E+02	0.055556
418.53	-5.00E-06	-8.66E-06	-1.20E+02	0.055325
412.835	-3.09E-06	-9.51E-06	-1.08E+02	0.054572
403.036	-1.05E-06	-9.95E-06	-9.60E+01	0.053276
389.025	1.05E-06	-9.95E-06	-8.40E+01	0.051424
371.063	3.09E-06	-9.51E-06	-7.20E+01	0.04905
349.004	5.00E-06	-8.66E-06	-6.00E+01	0.046134
323.514	6.69E-06	-7.43E-06	-4.80E+01	0.042765
296.179	8.09E-06	-5.88E-06	-3.60E+01	0.03915
268.568	9.14E-06	-4.07E-06	-2.40E+01	0.035501
243.251	9.78E-06	-2.08E-06	-1.20E+01	0.032155
221.848	1.00E-05	0	0.00E+00	0.029326
205.182	9.78E-06	2.08E-06	1.20E+01	0.027123
193.915	9.14E-06	4.07E-06	2.40E+01	0.025633
187.214	8.09E-06	5.88E-06	3.60E+01	0.024747
184.447	6.69E-06	7.43E-06	4.80E+01	0.024382
186.363	5.00E-06	8.66E-06	6.00E+01	0.024635
193.258	3.09E-06	9.51E-06	7.20E+01	0.025546
205.235	1.05E-06	9.95E-06	8.40E+01	0.02713
222.596	-1.05E-06	9.95E-06	9.60E+01	0.029424
244.726	-3.09E-06	9.51E-06	1.08E+02	0.03235
270.282	-5.00E-06	8.66E-06	1.20E+02	0.035728
297.418	-6.69E-06	7.43E-06	1.32E+02	0.039315
324.173	-8.09E-06	5.88E-06	1.44E+02	0.042852
349.039	-9.14E-06	4.07E-06	1.56E+02	0.046139
370.746	-9.78E-06	2.08E-06	1.68E+02	0.049008

Table –2: Nu for various angles over front wire in 4-wire analyses at Re=0.015

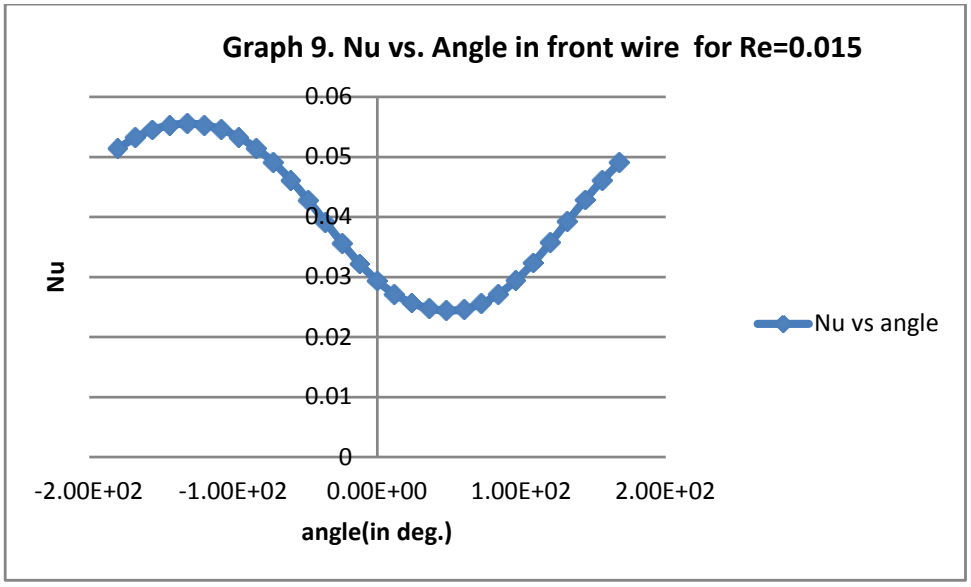
Graph 9. Nu vs. Angle in front wire for Re=0.015
0.06
0.05
0.04
0.03
0.02
0.01
0
Nu
-2.00E+02
-1.00E+02
0.00E+00
1.00E+02
2.00E+02
angle(in deg.)
Nu vs angle

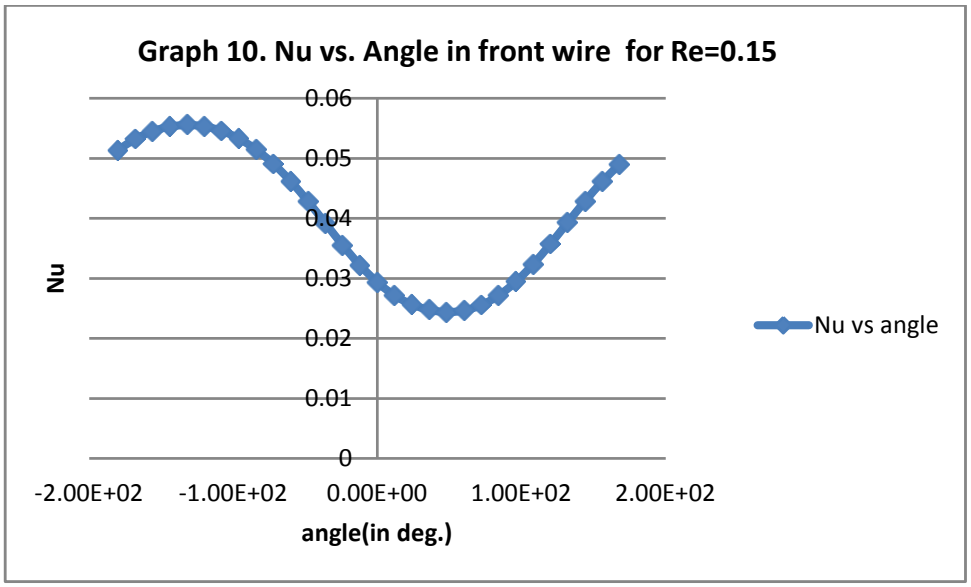
Graph 10. Nu vs. Angle in front wire for Re=0.15
0.06
0.05
0.04
0.03
0.02
0.01
0
Nu
-2.00E+02
-1.00E+02
0.00E+00
1.00E+02
2.00E+02
angle(in deg.)
Nu vs angle

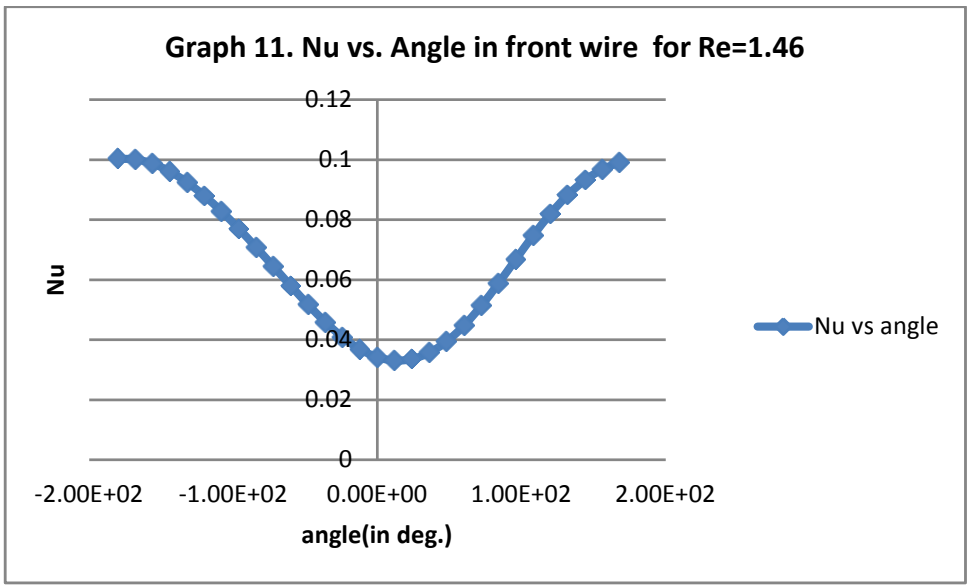
Graph 11. Nu vs. Angle in front wire for Re=1.46
0.12
0.1
0.08
0.06
0.04
0.02
0
Nu
-2.00E+02
-1.00E+02
0.00E+00
1.00E+02
2.00E+02
angle(in deg.)
Nu vs angle

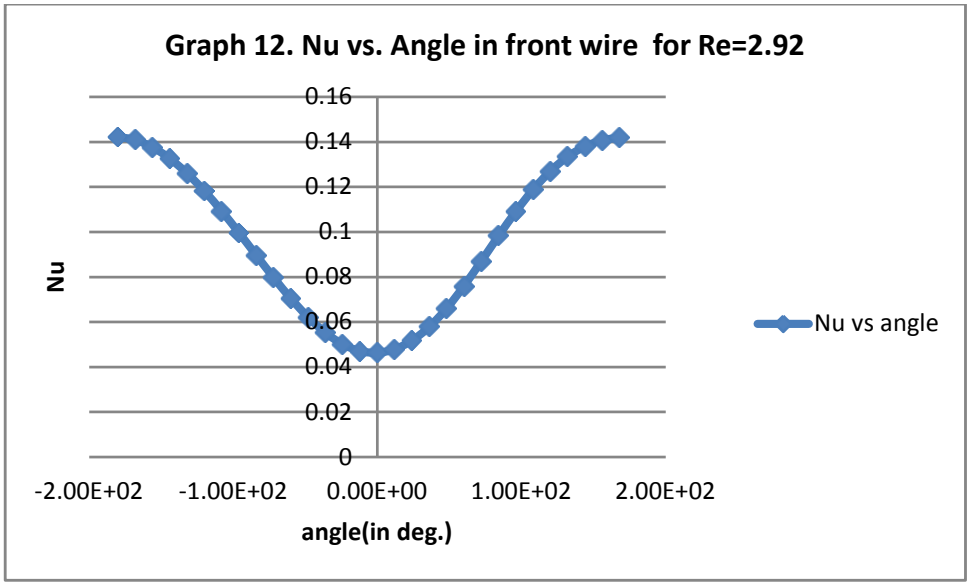
Graph 12. Nu vs. Angle in front wire for Re=2.92
0.16
0.14
0.12
0.1
0.08
0.06
0.04
0.02
0
Nu
-2.00E+02
-1.00E+02
0.00E+00
1.00E+02
2.00E+02
angle(in deg.)
Nu vs angle

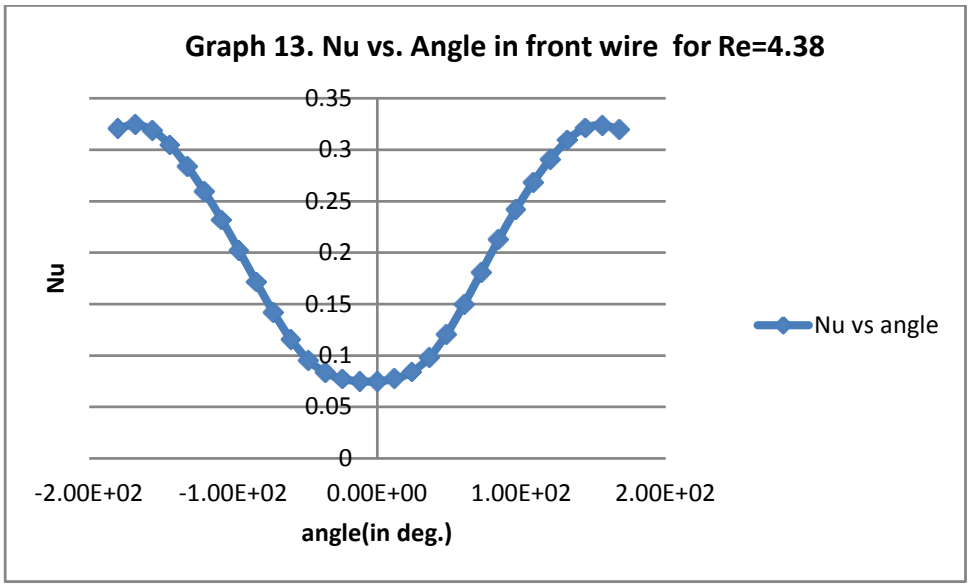
Graph 13. Nu vs. Angle in front wire for Re=4.38
0.35
0.3
0.25
0.2
0.15
0.1
0.05
0
Nu
-2.00E+02
-1.00E+02
0.00E+00
1.00E+02
2.00E+02
angle(in deg.)
Nu vs angle

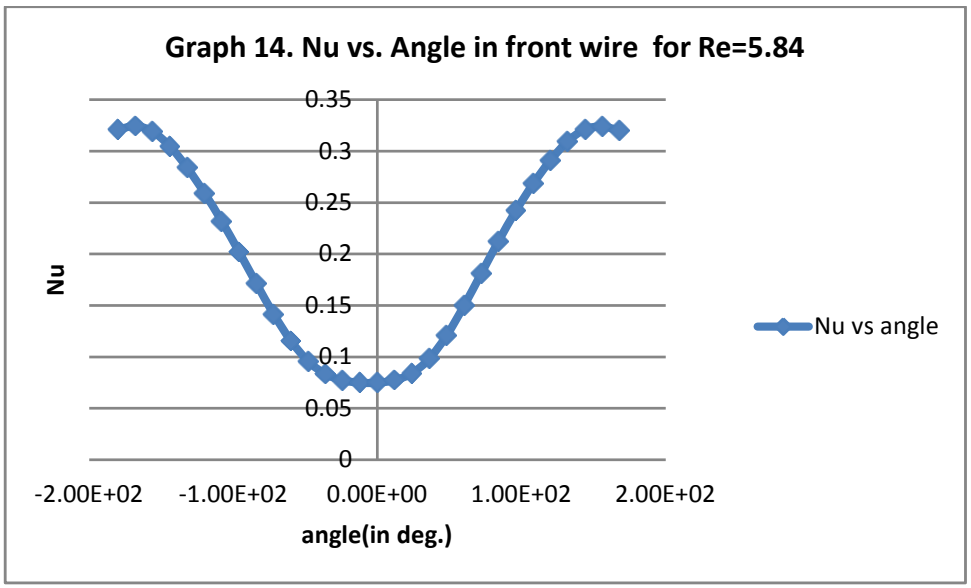
Graph 14. Nu vs. Angle in front wire for Re=5.84
0.35
0.3
0.25
0.2
0.15
0.1
0.05
0
Nu
-2.00E+02
-1.00E+02
0.00E+00
1.00E+02
2.00E+02
angle(in deg.)
Nu vs angle

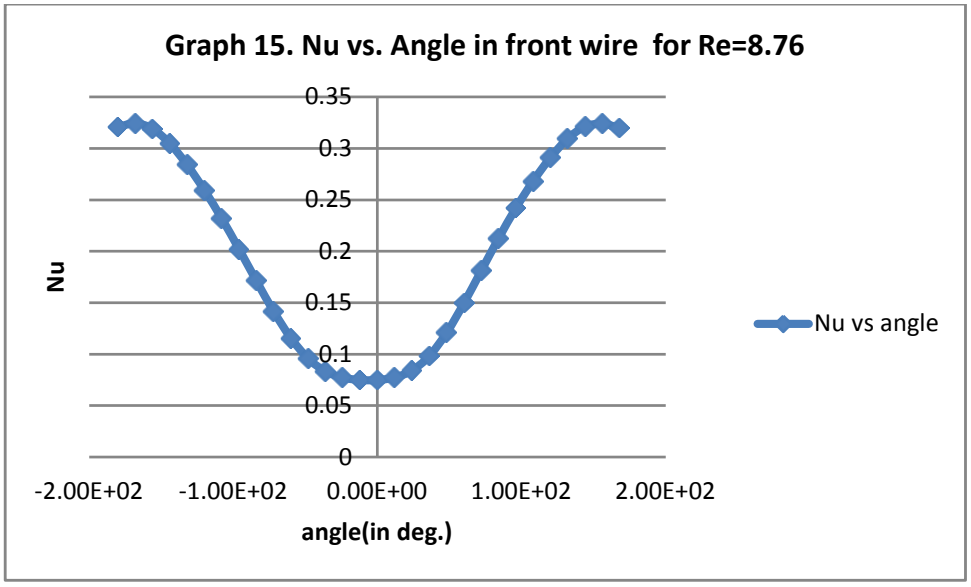

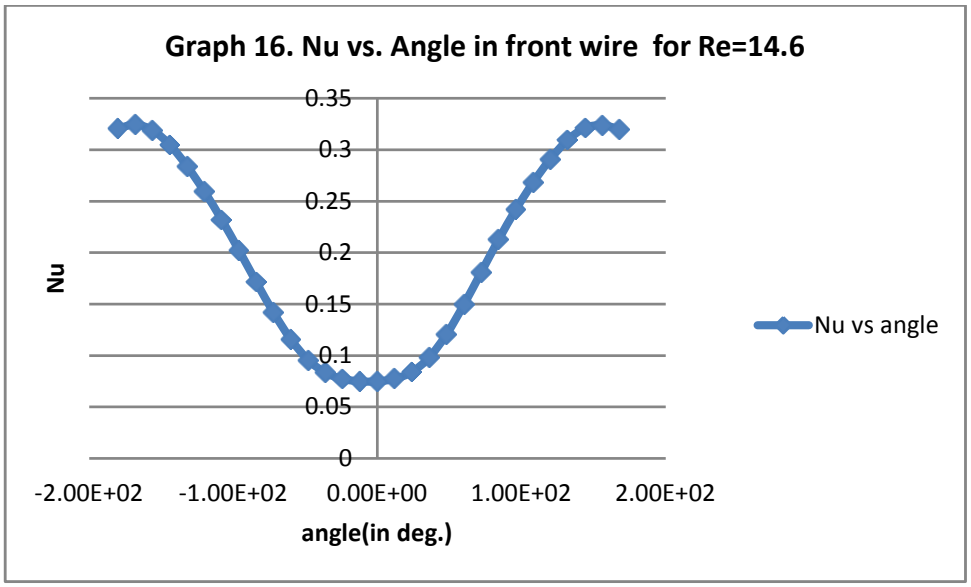

Graphs of Nusselt number (Nu) vs. Angle gave a deep insight into the change of Nusselt number over a surface. Minimum Nusselt number occurred at a point. The four wire analysis gives very interesting results. The wires at the front had a similar flow pattern throughout with very little change in the point of minimum Nu. The shift was slowly towards angle (θ) $=0^{o}$. The variation is sinusoidal as shown

The wires at the back however showed a greater change in point of minimum Nu with Re. The table below shows Nu for various angles on the rear cylinder for Re=0.015. the graphs were plotted for Nu vs. Angle for each Re.

Surface Heat Transfer Coef.	x	y	Angle (in deg.)	Nu
226.527	5.35E-05	-5.67E-21	-1.80E+02	0.029944
248.081	5.37E-05	-2.08E-06	-1.68E+02	0.032793
273.821	5.44E-05	-4.07E-06	-1.56E+02	0.036196
302.415	5.54E-05	-5.88E-06	-1.44E+02	0.039976
331.608	5.68E-05	-7.43E-06	-1.32E+02	0.043835
359.208	5.85E-05	-8.66E-06	-1.20E+02	0.047483
383.974	6.04E-05	-9.51E-06	-1.08E+02	0.050757
404.801	6.25E-05	-9.95E-06	-9.60E+01	0.05351
421.429	6.45E-05	-9.95E-06	-8.40E+01	0.055708
433.712	6.66E-05	-9.51E-06	-7.20E+01	0.057331
441.682	6.85E-05	-8.66E-06	-6.00E+01	0.058385
445.43	7.02E-05	-7.43E-06	-4.80E+01	0.05888
445.182	7.16E-05	-5.88E-06	-3.60E+01	0.058848
440.602	7.26E-05	-4.07E-06	-2.40E+01	0.058242
431.923	7.33E-05	-2.08E-06	-1.20E+01	0.057095
418.912	7.35E-05	0	0.00E+00	0.055375
400.659	7.33E-05	2.08E-06	1.20E+01	0.052962
378.328	7.26E-05	4.07E-06	2.40E+01	0.05001
352.401	7.16E-05	5.88E-06	3.60E+01	0.046583
323.989	7.02E-05	7.43E-06	4.80E+01	0.042827
294.794	6.85E-05	8.66E-06	6.00E+01	0.038968
266.676	6.66E-05	9.51E-06	7.20E+01	0.035251
241.687	6.45E-05	9.95E-06	8.40E+01	0.031948
221.302	6.25E-05	9.95E-06	9.60E+01	0.029253
206.29	6.04E-05	9.51E-06	1.08E+02	0.027269
196.753	5.85E-05	8.66E-06	1.20E+02	0.026008
192.438	5.68E-05	7.43E-06	1.32E+02	0.025438
193.063	5.54E-05	5.88E-06	1.44E+02	0.025521
198.882	5.44E-05	4.07E-06	1.56E+02	0.02629
210.025	5.37E-05	2.08E-06	1.68E+02	0.027763

Table –3: Nu for various angles over 2nd wire in 4-wire analyses at Re=0.015

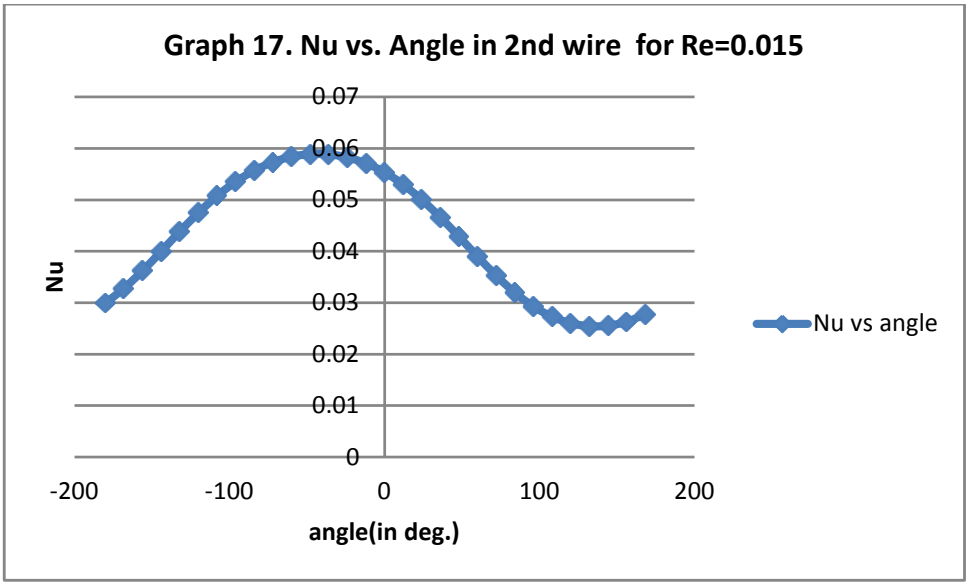
Graph 17. Nu vs. Angle in 2nd wire for Re=0.015
0.07
0.06
0.05
0.04
0.03
0.02
0.01
0
Nu
-200
-100
0
100
200
angle(in deg.)
Nu vs angle

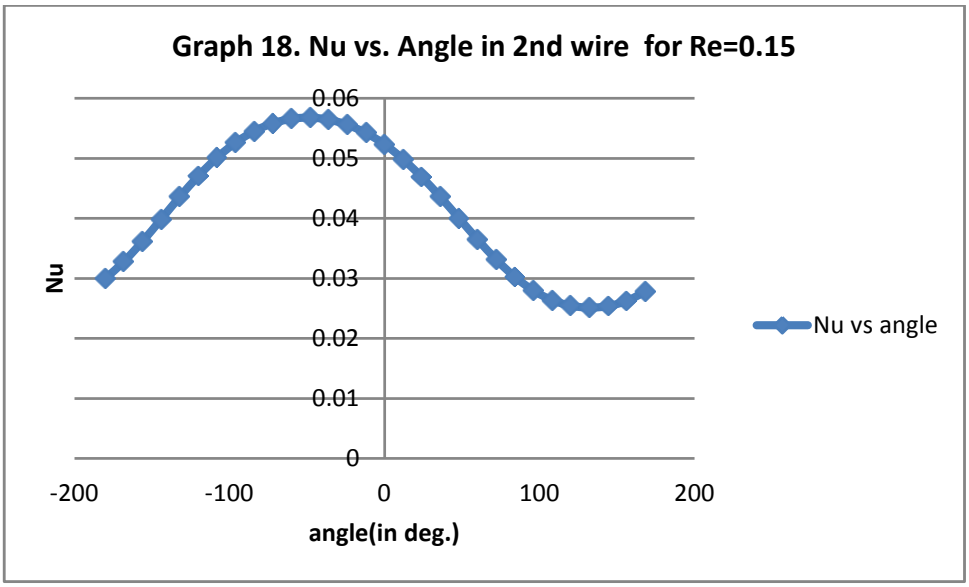
Graph 18. Nu vs. Angle in 2nd wire for Re=0.15
0.06
0.05
0.04
0.03
0.02
0.01
0
Nu
-200
-100
0
100
200
angle(in deg.)
Nu vs angle

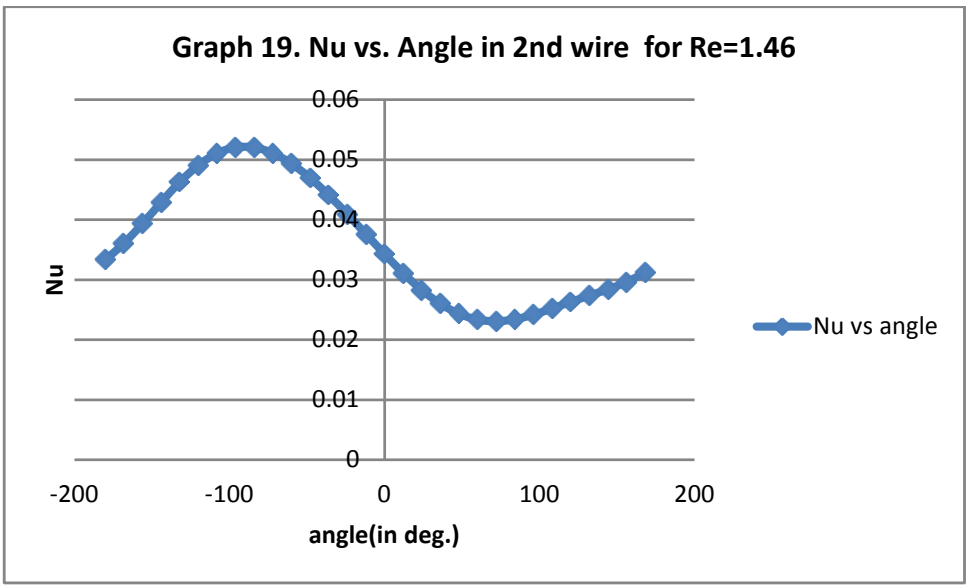
Graph 19. Nu vs. Angle in 2nd wire for Re=1.46
0.06
0.05
0.04
0.03
0.02
0.01
0
Nu
-200
-100
0
100
200
angle(in deg.)
Nu vs angle

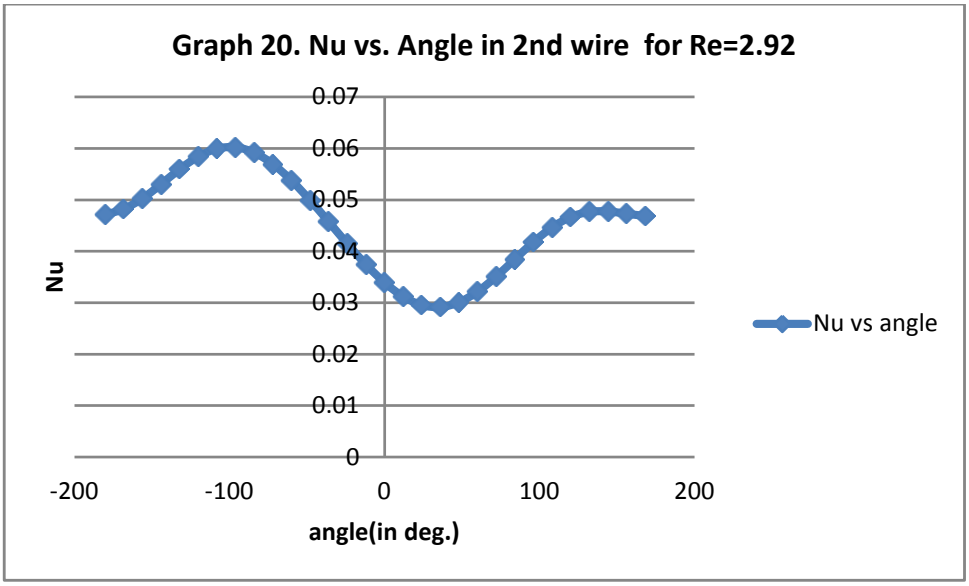
Graph 20. Nu vs. Angle in 2nd wire for Re=2.92
0.07
0.06
0.05
0.04
0.03
0.02
0.01
0
Nu
-200
-100
0
100
200
angle(in deg.)
Nu vs angle

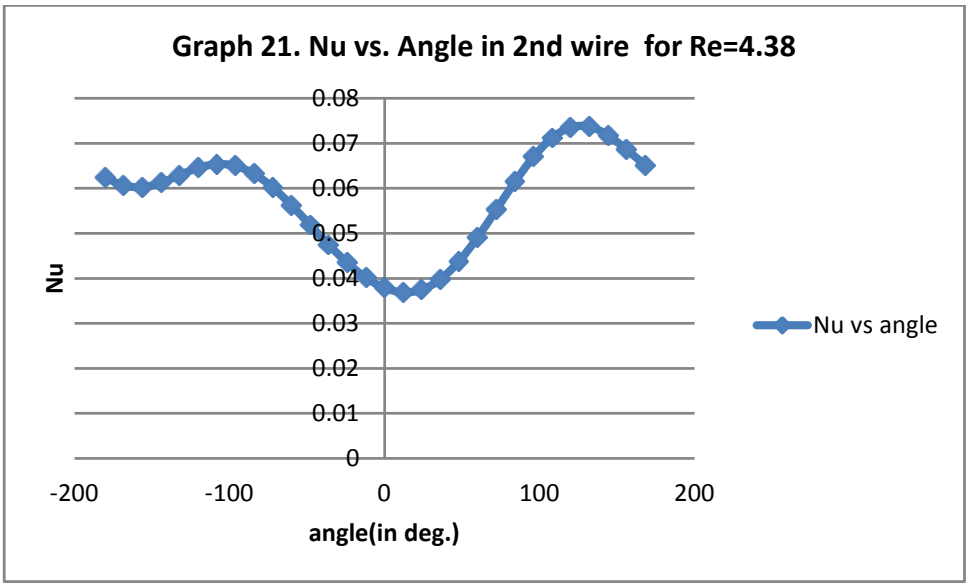
Graph 21. Nu vs. Angle in 2nd wire for Re=4.38
0.08
0.07
0.06
0.05
0.04
0.03
0.02
0.01
0
Nu
-200
-100
0
100
200
angle(in deg.)
Nu vs angle

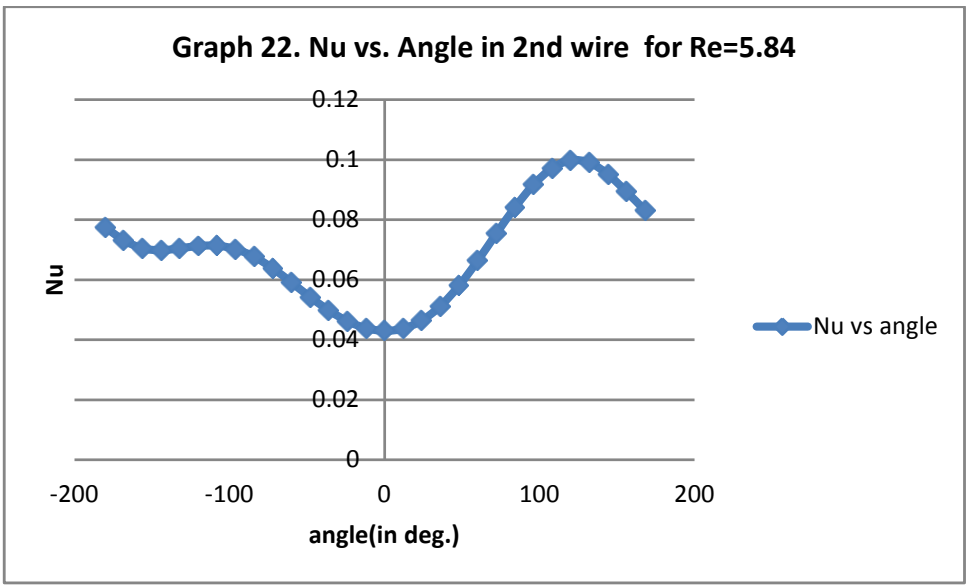
Graph 22. Nu vs. Angle in 2nd wire for Re=5.84
0.12
0.1
0.08
0.06
0.04
0.02
0
Nu
-200
-100
0
100
200
angle(in deg.)
Nu vs angle

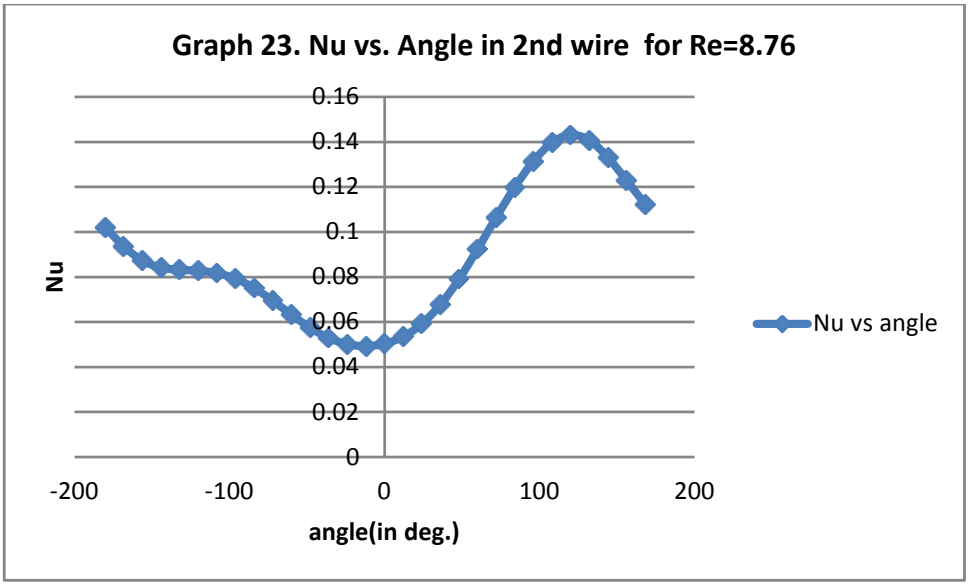

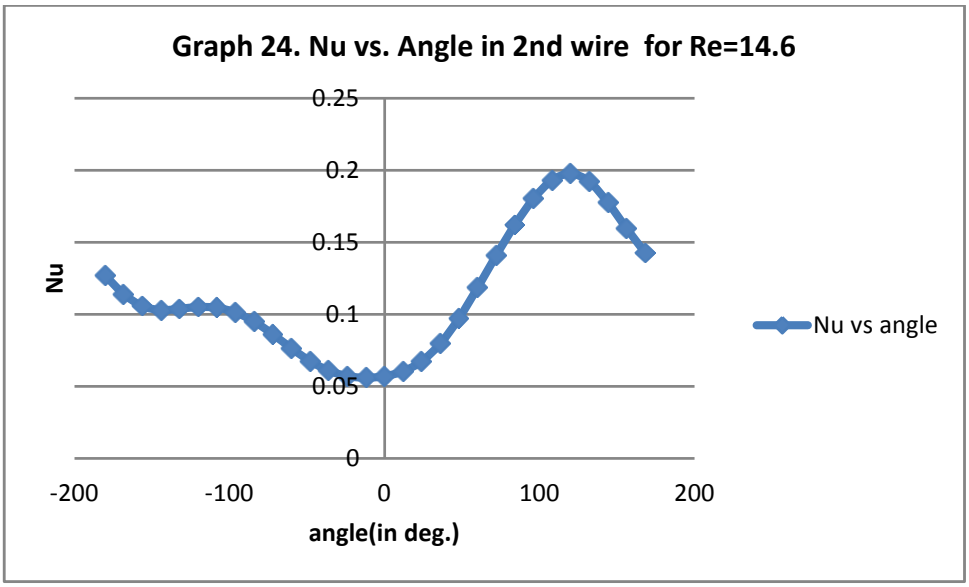

For low values of Re, one maxima was observed. When the Re was increased gradually, the number of maxima increased to 2. For higher values of Re, the number of maxima again became 1 but they were observed for positive values of angle unlike for low Re where they were in the negative side.

For low values of Re, the point of minimum Nu was at the upper part of the cylinder ($\theta=132^{o}$ for Re=0.015). As Re increased, the point shifted to back of the cylinder. The variation of angle of minimum Nu vs. Re is shown below.

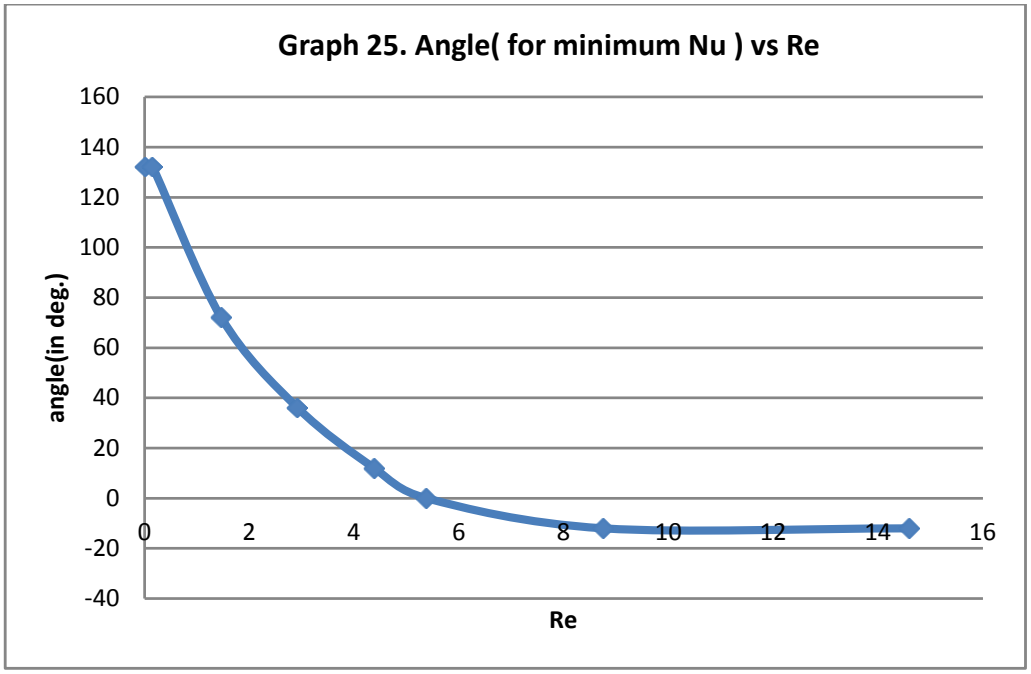
Graph 25. Angle(for minimum Nu) vs Re
160
140
120
100
80
60
40
20
0
-20
-40
angle(in deg.)
0
2
4
6
8
10
12
14
16
Re

CHAPTER-7

NINE WIRE ANALYSES

Four wire analyses considered fluid flow in symmetric condition. There was no central cylinder on which fluid flow effects could be studied. The effect of side cylinder could not be observed. So the study of effects of side cylinders necessitates the analysis of nine wires in an inline arrangement. The wire system gives a clear picture of the fluid flow in a multi wire system where the effects of side cylinders affect the heat absorption and consequently the Nusselt number.

In a 9 wire system, the flow over the central row of wires is of special importance as they have a different pattern of flow due to the presence of other wires at the sides.

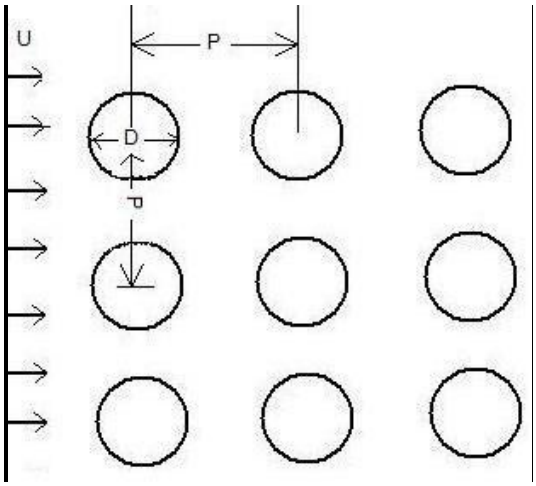

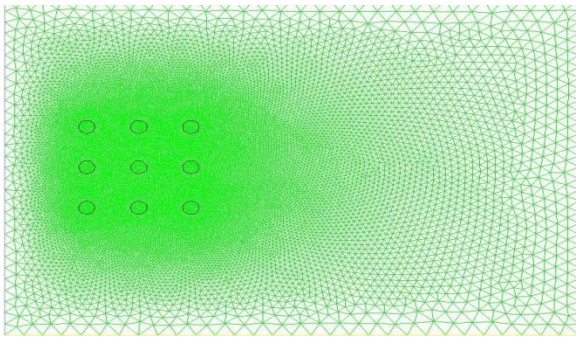

Fig.12 Real geometry Fig.13 Mesh geometry

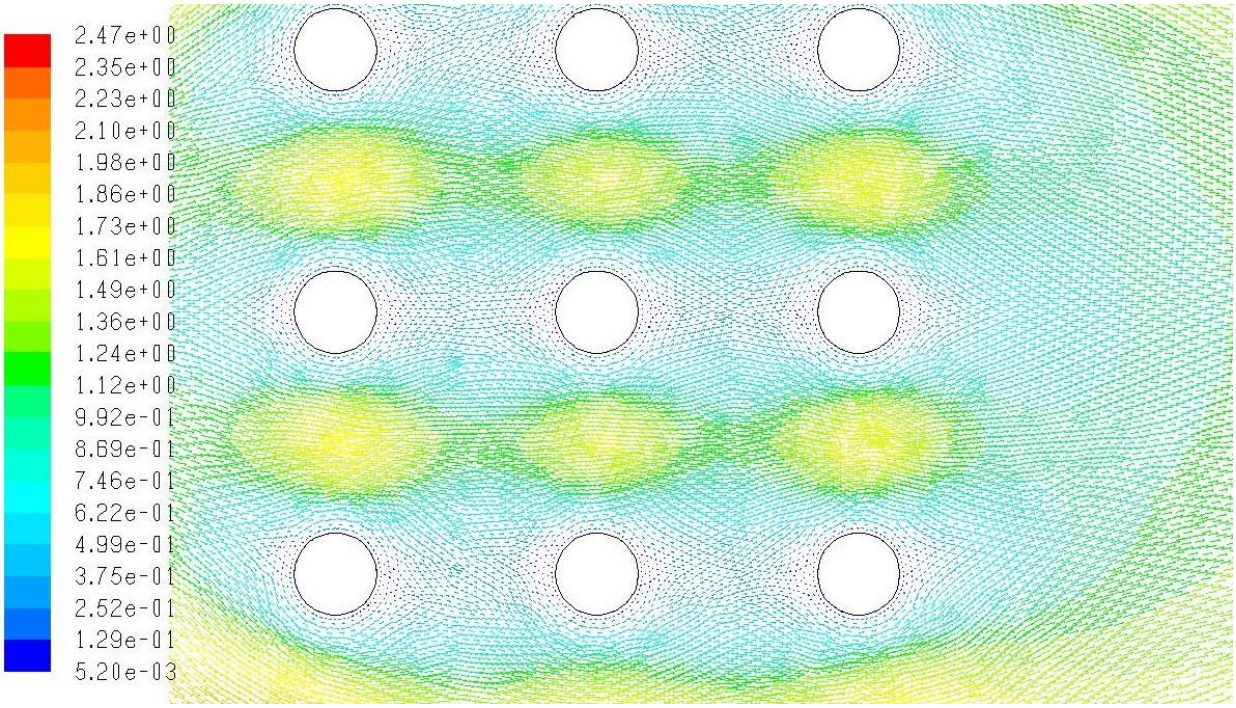

Fig.14 Velocity vector (in ms^{-1})

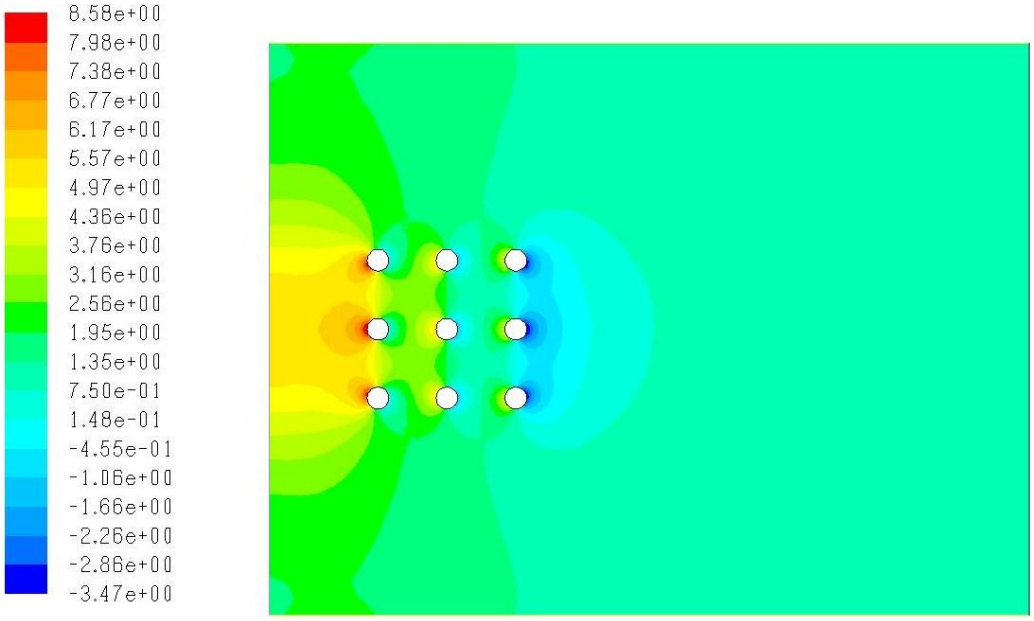

Fig.15 Pressure contour (in atm)

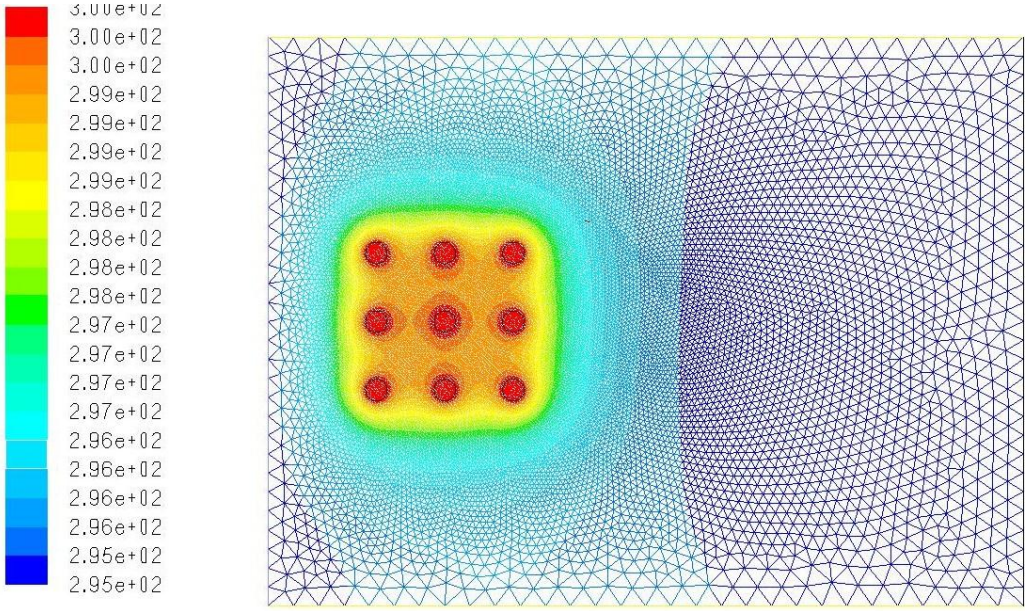

Fig.16 Temperature contour (in Kelvin)

Here the pitch (p) was taken to be $63.5X10^{-6}$ m. The diameter of the wire (D) was taken as $20X10^{-6}$ m. The analysis mainly concentrates its focus on the middle row of cylinders with special attention the 2nd cylinder.

Considering the 1st cylinder in the 2nd row, the data for Re=0.015 is shown in the table below. Subsequently graphs of angle vs. Nu were plotted for various

Surface Heat Transfer Coef.	x	y	Angle (in deg.)	Nu
2297.53	-1.00E-05	-1.22E-21	-1.80E+02	0.151853
2386.68	-9.78E-06	-2.08E-06	-1.68E+02	0.157745
2450.43	-9.14E-06	-4.07E-06	-1.56E+02	0.161958
2488.19	-8.09E-06	-5.88E-06	-1.44E+02	0.164454
2500.36	-6.69E-06	-7.43E-06	-1.32E+02	0.165258
2486.83	-5.00E-06	-8.66E-06	-1.20E+02	0.164364
2447.86	-3.09E-06	-9.51E-06	-1.08E+02	0.161788
2382.57	-1.05E-06	-9.95E-06	-9.60E+01	0.157473
2291.59	1.05E-06	-9.95E-06	-8.40E+01	0.15146
2174.51	3.09E-06	-9.51E-06	-7.20E+01	0.143722
2028	5.00E-06	-8.66E-06	-6.00E+01	0.134038
1863.28	6.69E-06	-7.43E-06	-4.80E+01	0.123151
1687.21	8.09E-06	-5.88E-06	-3.60E+01	0.111514
1510.14	9.14E-06	-4.07E-06	-2.40E+01	0.099811
1346.28	9.78E-06	-2.08E-06	-1.20E+01	0.088981
1205.19	1.00E-05	0	0.00E+00	0.079656
1094.1	9.78E-06	2.08E-06	1.20E+01	0.072313
1015.72	9.14E-06	4.07E-06	2.40E+01	0.067133
971.135	8.09E-06	5.88E-06	3.60E+01	0.064186
959.912	6.69E-06	7.43E-06	4.80E+01	0.063444
977.649	5.00E-06	8.66E-06	6.00E+01	0.064617
1025.69	3.09E-06	9.51E-06	7.20E+01	0.067792
1108.51	1.05E-06	9.95E-06	8.40E+01	0.073266
1224.05	-1.05E-06	9.95E-06	9.60E+01	0.080902
1369.18	-3.09E-06	9.51E-06	1.08E+02	0.090494
1534.13	-5.00E-06	8.66E-06	1.20E+02	0.101397
1708.79	-6.69E-06	7.43E-06	1.32E+02	0.112941
1882.2	-8.09E-06	5.88E-06	1.44E+02	0.124402
2042.29	-9.14E-06	4.07E-06	1.56E+02	0.134983
2181.83	-9.78E-06	2.08E-06	1.68E+02	0.144206

Table –4: Nu for various angles over front wire in 9-wire analyses at Re=0.015

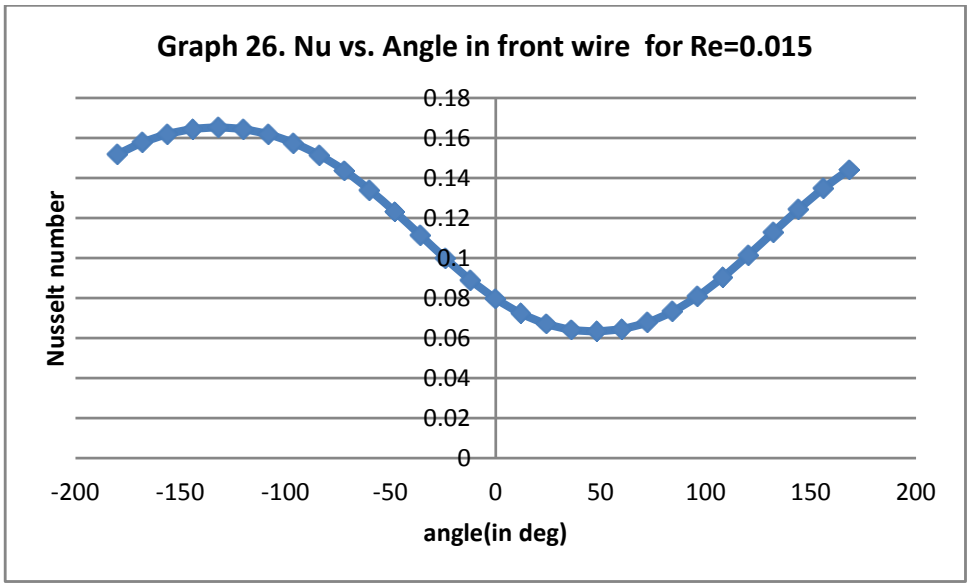
Graph 26. Nu vs. Angle in front wire for Re=0.015
Nusselt number
0.18
0.16
0.14
0.12
0.1
0.08
0.06
0.04
0.02
0
-200
-150
-100
-50
0
50
100
150
200
angle(in deg)

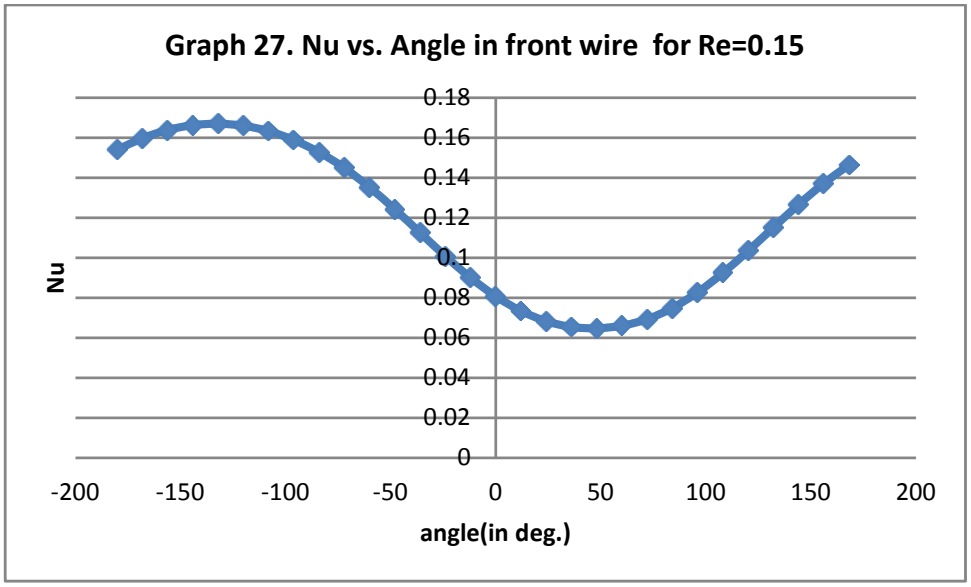
Graph 27. Nu vs. Angle in front wire for Re=0.15
Nu
0.18
0.16
0.14
0.12
0.1
0.08
0.06
0.04
0.02
0
-200
-150
-100
-50
0
50
100
150
200
angle(in deg.)

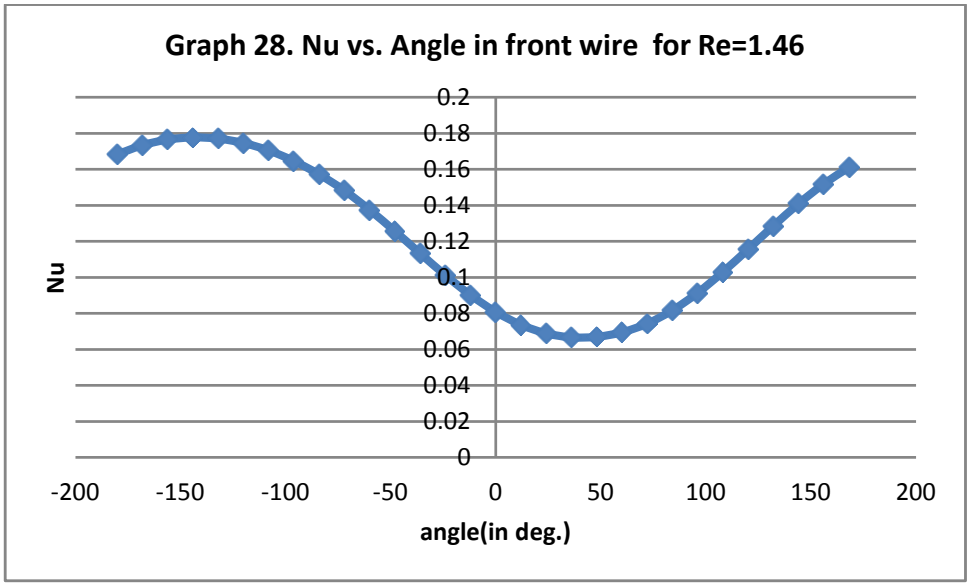
Graph 28. Nu vs. Angle in front wire for Re=1.46
Nu
0.2
0.18
0.16
0.14
0.12
0.1
0.08
0.06
0.04
0.02
0
-200
-150
-100
-50
0
50
100
150
200
angle(in deg.)

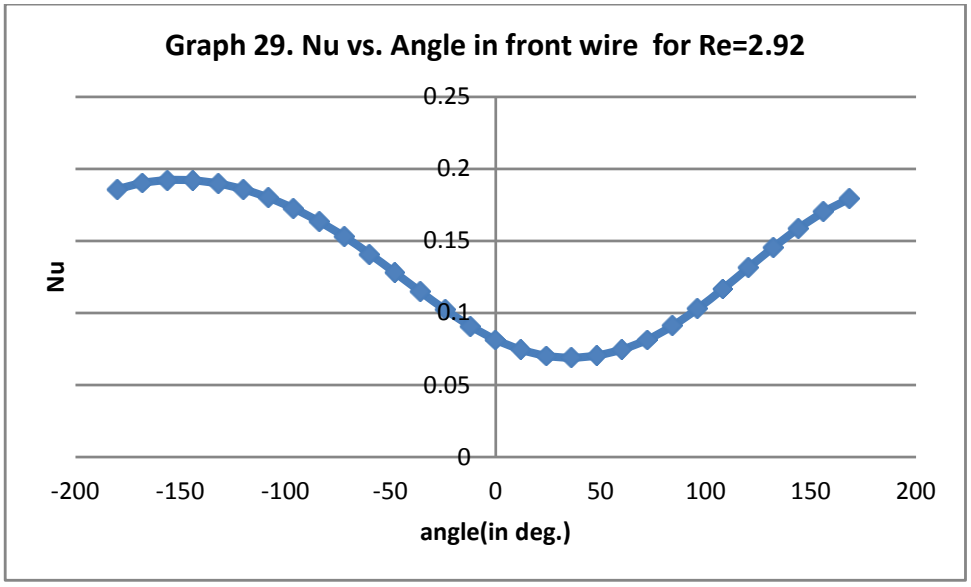
Graph 29. Nu vs. Angle in front wire for Re=2.92
0.25
0.2
0.15
0.1
0.05
0
Nu
-200
-150
-100
-50
0
50
100
150
200
angle(in deg.)

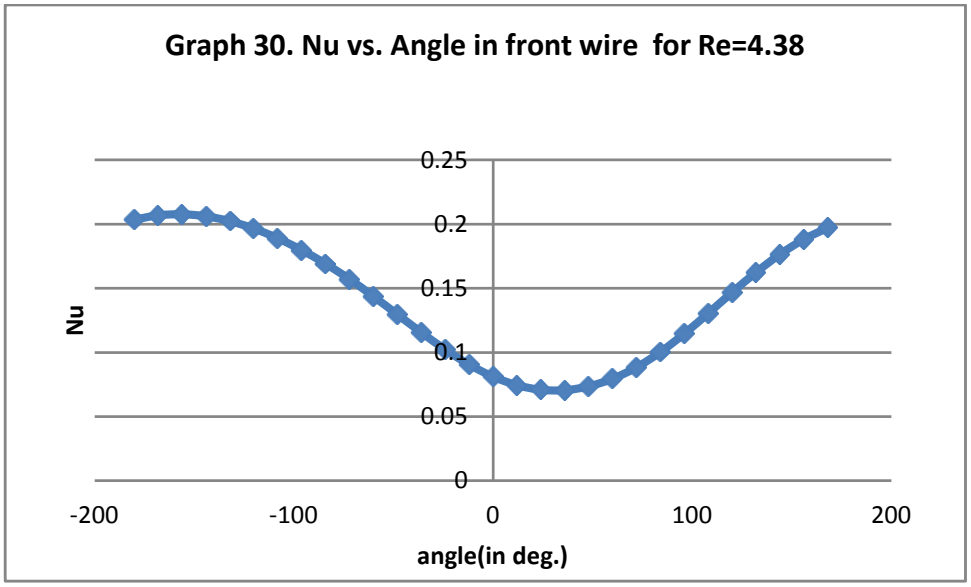
Graph 30. Nu vs. Angle in front wire for Re=4.38
0.25
0.2
0.15
0.1
0.05
0
Nu
-200
-100
0
100
200
angle(in deg.)

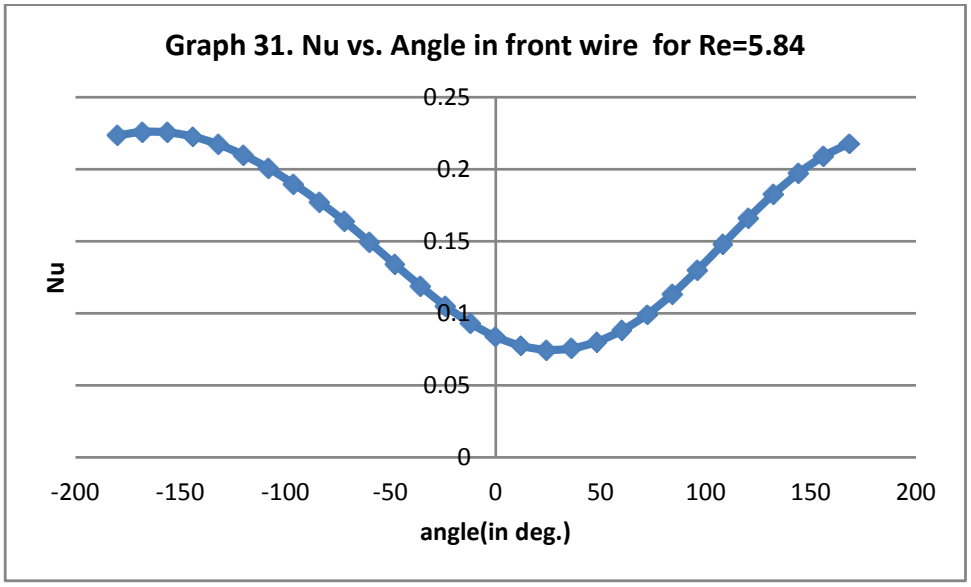
Graph 31. Nu vs. Angle in front wire for Re=5.84
0.25
0.2
0.15
0.1
0.05
0
Nu
-200
-150
-100
-50
0
50
100
150
200
angle(in deg.)

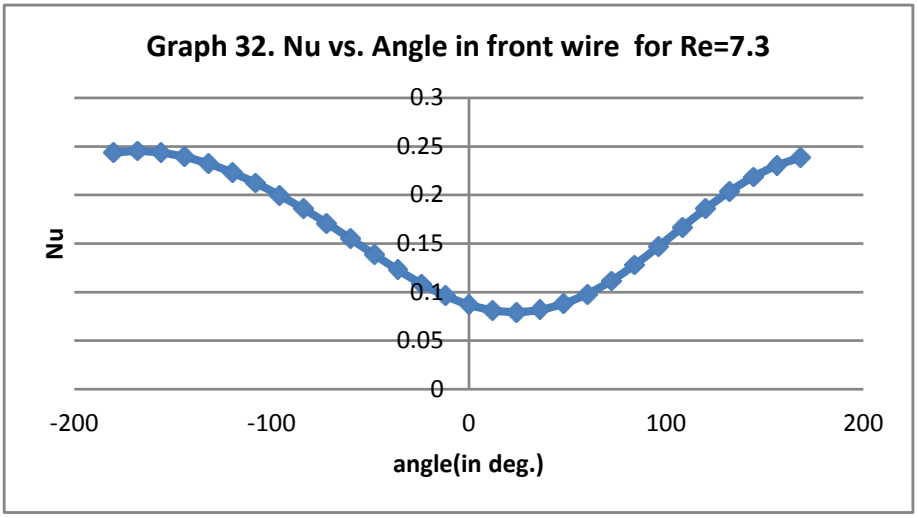

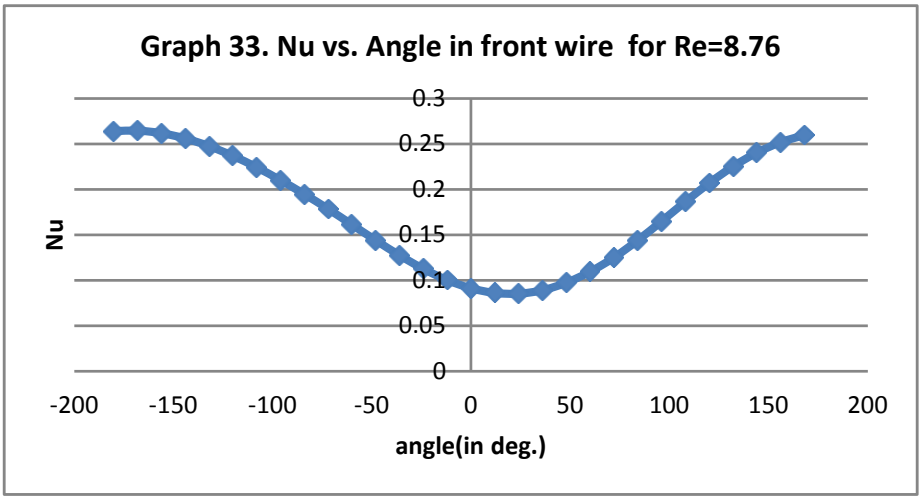

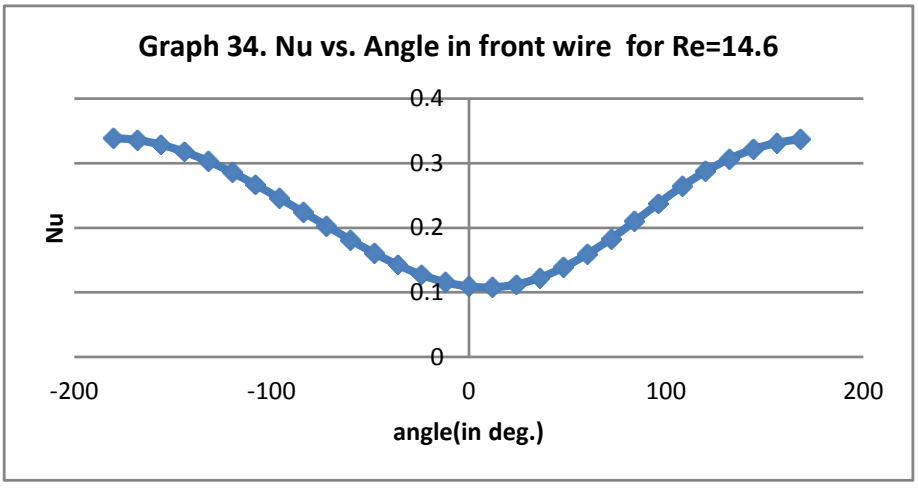

As can be seen, the value shows a similar trend throughout with a gradual increase in the maximum value and the minimum values. The graph seems to rise with increase in Re.

For the 2nd cylinder, the values of angle and Nu for Re = 0.015 is shown below.

Surface Heat Transfer Coef.	x	y	Angle (in deg.)	Nu
1181.56	5.35E-05	-5.67E-21	-180.091	0.078094
1322.93	5.37E-05	-2.08E-06	-168.085	0.087438
1479.97	5.44E-05	-4.07E-06	-156.079	0.097817
1641.53	5.54E-05	-5.88E-06	-144.073	0.108495
1793.85	5.68E-05	-7.43E-06	-132.067	0.118562
1922.86	5.85E-05	-8.66E-06	-120.061	0.127089
2017.39	6.04E-05	-9.51E-06	-108.055	0.133337
2069.32	6.25E-05	-9.95E-06	-96.0488	0.136769
2074.18	6.45E-05	-9.95E-06	-84.0425	0.137091
2033.45	6.66E-05	-9.51E-06	-72.0364	0.134399
1949.69	6.85E-05	-8.66E-06	-60.0304	0.128863
1829.48	7.02E-05	-7.43E-06	-48.0244	0.120917
1683.71	7.16E-05	-5.88E-06	-36.0181	0.111283
1526.7	7.26E-05	-4.07E-06	-24.0121	0.100905
1371.51	7.33E-05	-2.08E-06	-12.0061	0.090648
1230.03	7.35E-05	0	0	0.081297
1109.78	7.33E-05	2.08E-06	12.00608	0.07335
1012.77	7.26E-05	4.07E-06	24.01209	0.066938
936.352	7.16E-05	5.88E-06	36.01815	0.061887
878.317	7.02E-05	7.43E-06	48.02438	0.058051
835.611	6.85E-05	8.66E-06	60.03042	0.055229
805.352	6.66E-05	9.51E-06	72.03636	0.053229
786.759	6.45E-05	9.95E-06	84.04252	0.052
779.586	6.25E-05	9.95E-06	96.04878	0.051526
787.315	6.04E-05	9.51E-06	108.0549	0.052037
809.727	5.85E-05	8.66E-06	120.0609	0.053518
846.473	5.68E-05	7.43E-06	132.0669	0.055947
898.472	5.54E-05	5.88E-06	144.0732	0.059383
969.01	5.44E-05	4.07E-06	156.079	0.064046
1062.64	5.37E-05	2.08E-06	168.0852	0.070234

Table –5: Nu for various angles over middle wire in 9-wire analyses at Re=0.015

Using the above data, the graph was plotted. Similarly, graphs for various Re were obtained as below from FLUENT analysis.

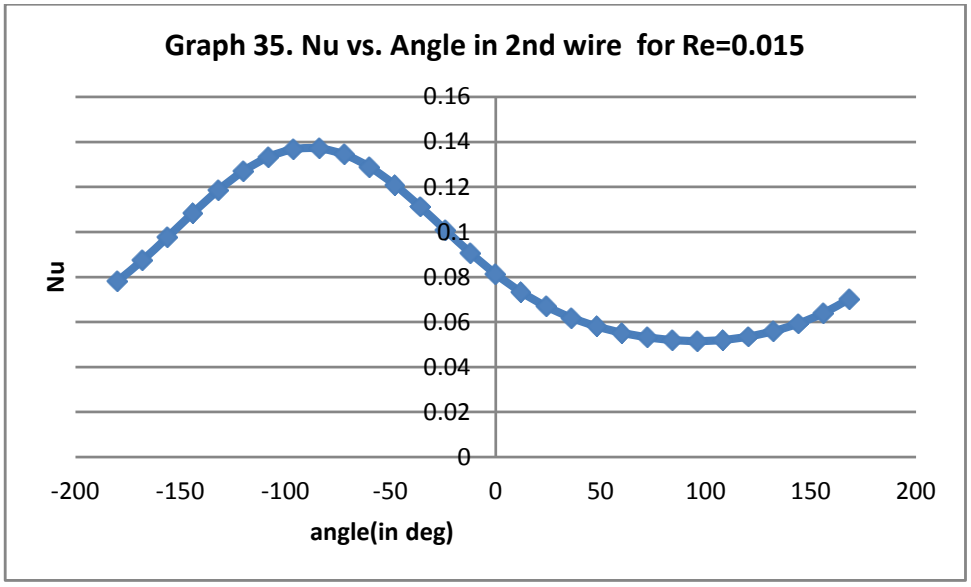

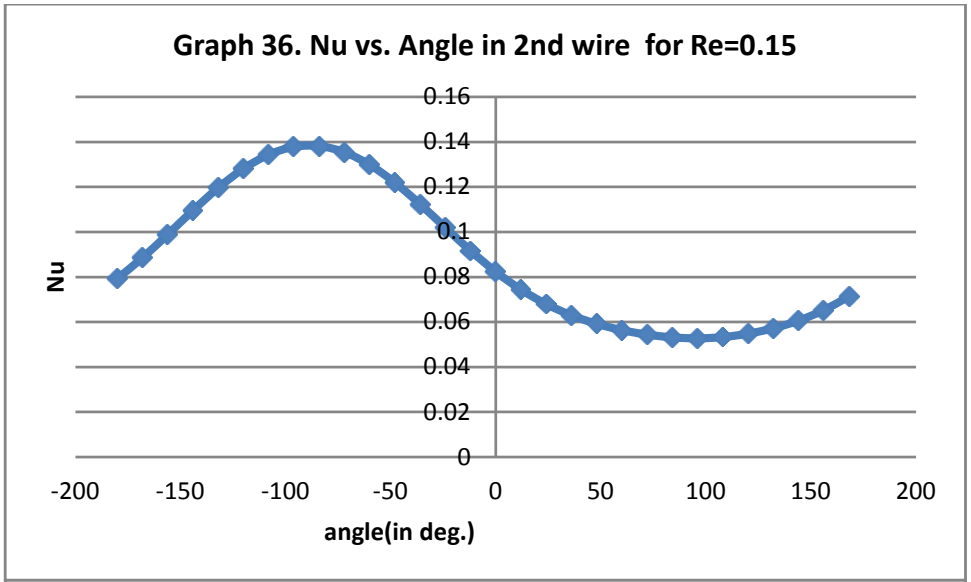
Graph 36. Nu vs. Angle in 2nd wire for Re=0.15
Nu
0.16
0.14
0.12
0.1
0.08
0.06
0.04
0.02
0
-200
-150
-100
-50
0
50
100
150
200
angle(in deg.)

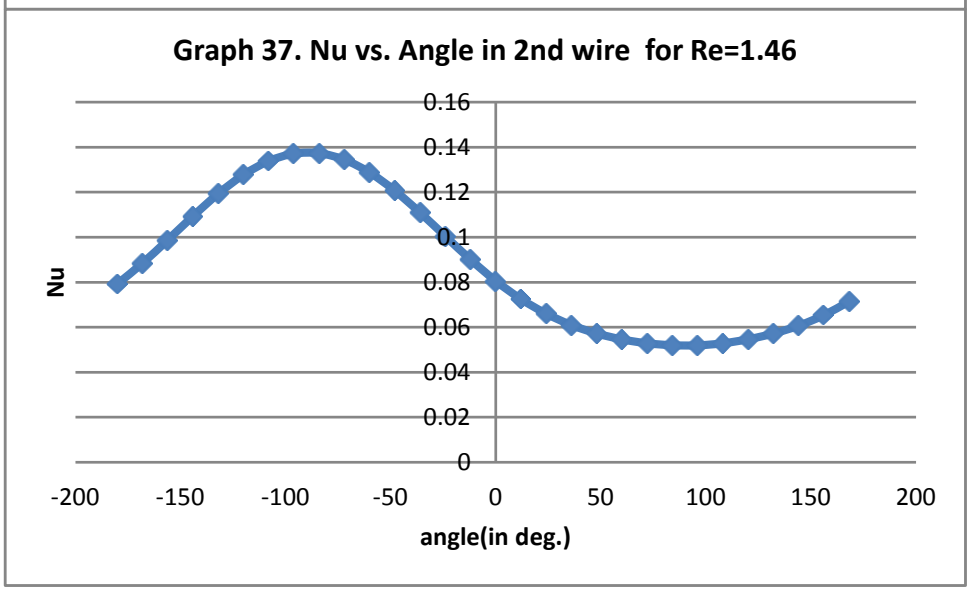
Graph 37. Nu vs. Angle in 2nd wire for Re=1.46
Nu
0.16
0.14
0.12
0.1
0.08
0.06
0.04
0.02
0
-200
-150
-100
-50
0
50
100
150
200
angle(in deg.)

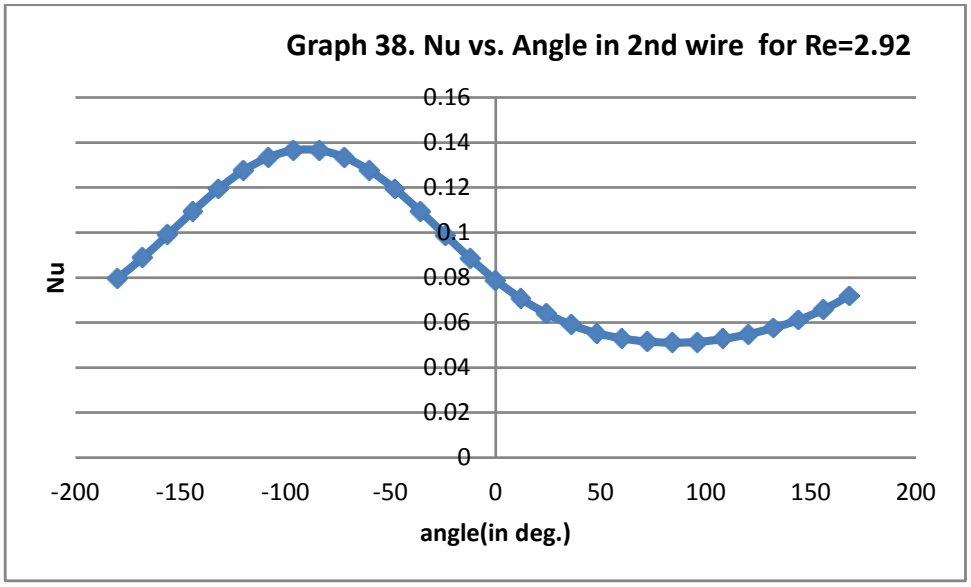
Graph 38. Nu vs. Angle in 2nd wire for Re=2.92
Nu
0.16
0.14
0.12
0.1
0.08
0.06
0.04
0.02
0
-200
-150
-100
-50
0
50
100
150
200
angle(in deg.)

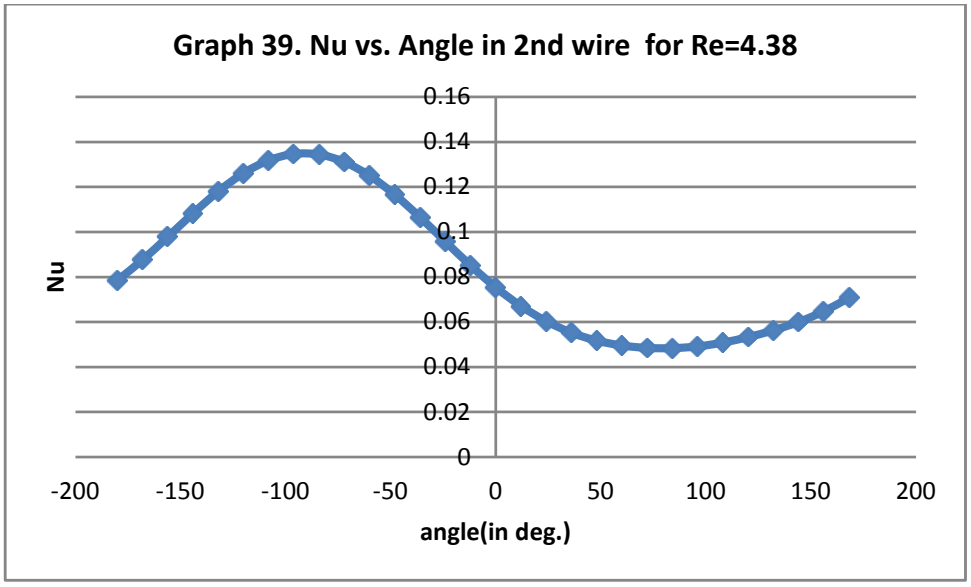
Graph 39. Nu vs. Angle in 2nd wire for Re=4.38
Nu
0.16
0.14
0.12
0.1
0.08
0.06
0.04
0.02
0
-200
-150
-100
-50
0
50
100
150
200
angle(in deg.)

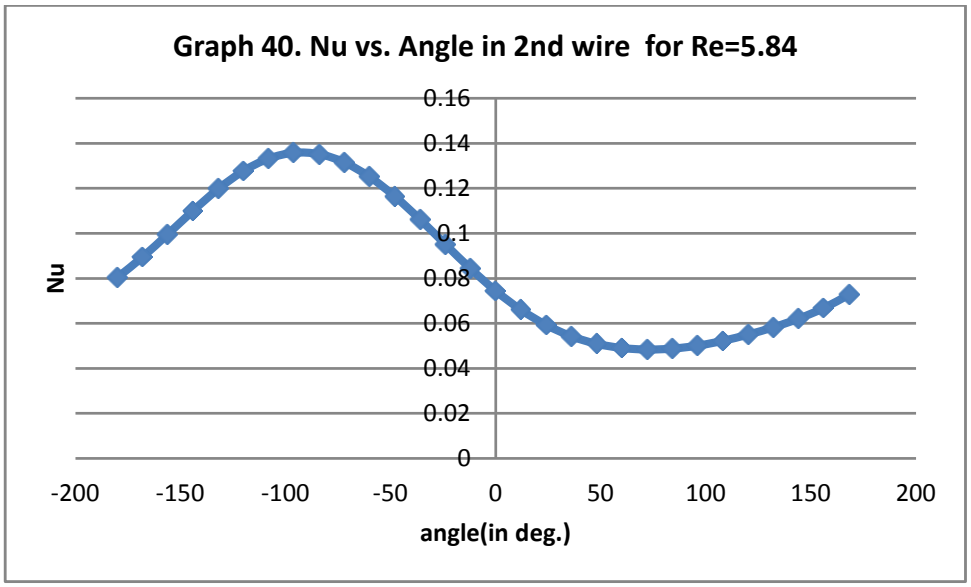
Graph 40. Nu vs. Angle in 2nd wire for Re=5.84
Nu
0.16
0.14
0.12
0.1
0.08
0.06
0.04
0.02
0
-200
-150
-100
-50
0
50
100
150
200
angle(in deg.)

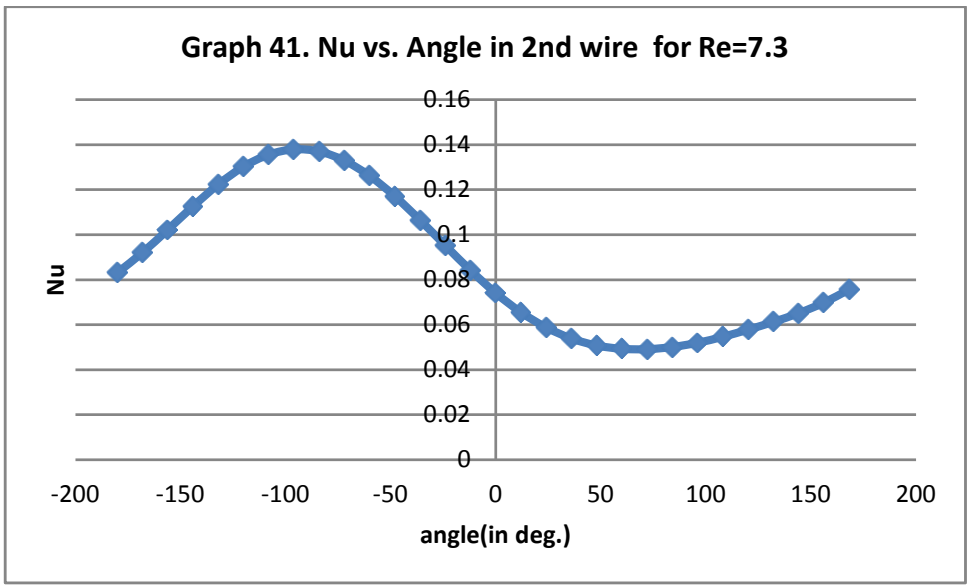
Graph 41. Nu vs. Angle in 2nd wire for Re=7.3
Nu
0.16
0.14
0.12
0.1
0.08
0.06
0.04
0.02
0
-200
-150
-100
-50
0
50
100
150
200
angle(in deg.)

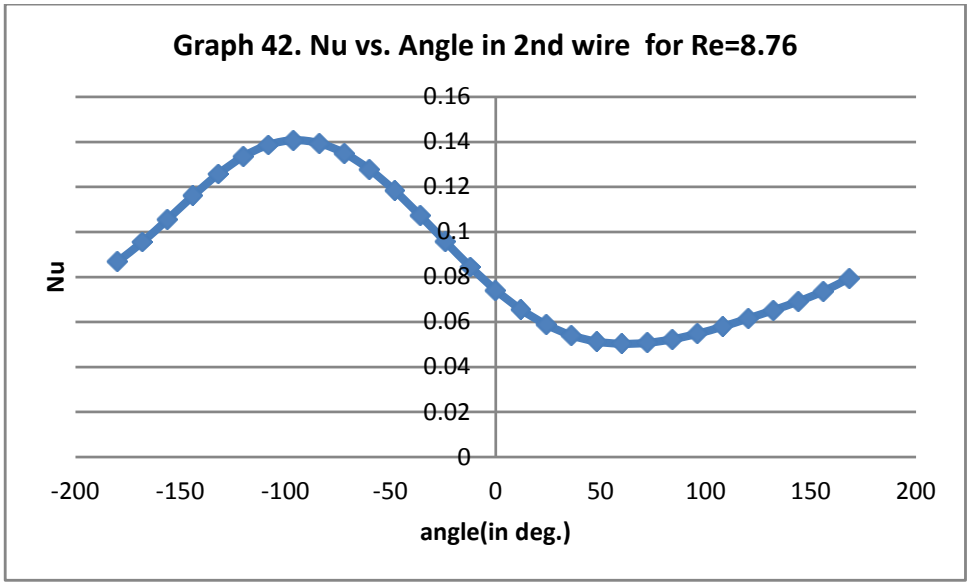

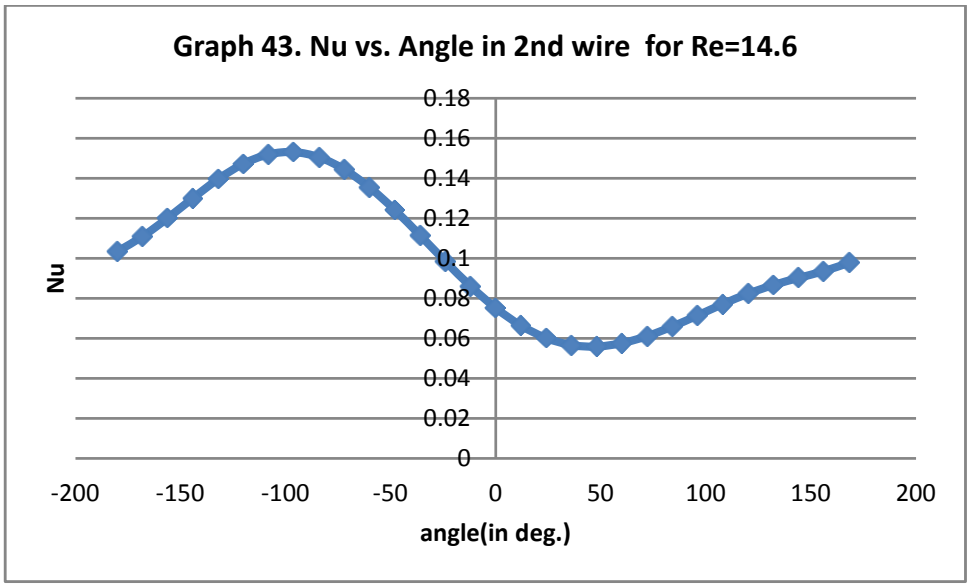

The graphs are similar in structure but the rise after the minima rises faster as Re increases. The values of Nu at maxima and minima are almost same in all the graphs. The minima is slowly shifting towards $\theta=0^0$. The graph below shows change in angle of minimum Nu vs. Re. This shows a slow shift in θ for very low Re (0.015-15).

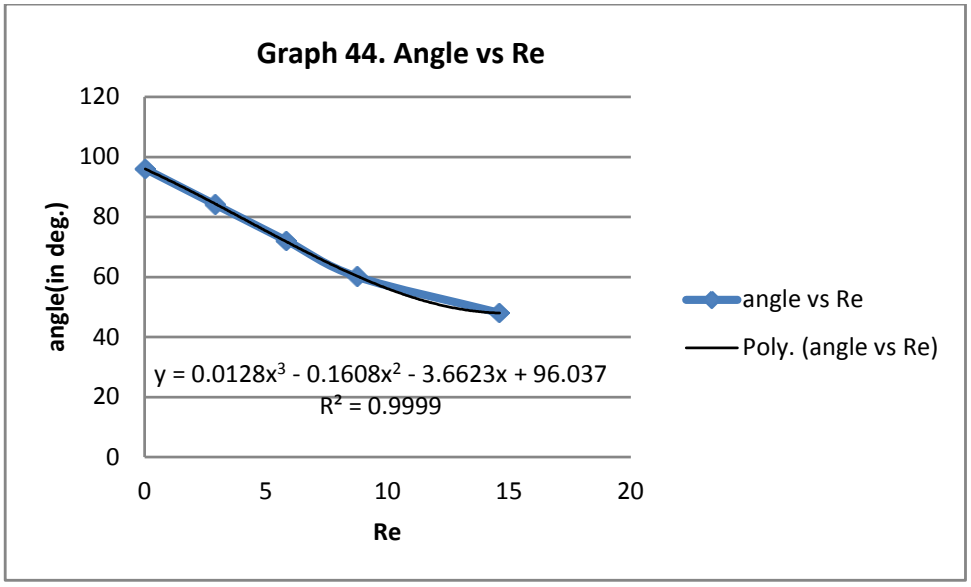
Graph 44. Angle vs Re
120
100
80
60
40
20
0
angle(in deg.)
0
5
10
15
20
Re
y = 0.0128x³ - 0.1608x² - 3.6623x + 96.037
R² = 0.9999
angle vs Re
Poly. (angle vs Re)

For the 3rd cylinder, similar data for angle vs. Nu (Re=0.015)is as follows:

Surface Heat Transfer Coef.	x	y	angle	Nu
1430.03	0.000117	-2.08E-06	-168.085	0.094516
1602.31	0.000118	-4.07E-06	-156.078	0.105903
1790.21	0.000119	-5.88E-06	-144.072	0.118322
1980.13	0.00012	-7.43E-06	-132.066	0.130874
2160.14	0.000122	-8.66E-06	-120.061	0.142772
2321.25	0.000124	-9.51E-06	-108.054	0.15342
2457.89	0.000126	-9.95E-06	-96.0471	0.162451
2567.48	0.000128	-9.95E-06	-84.0442	0.169695
2649.74	0.00013	-9.51E-06	-72.0375	0.175132
2705.29	0.000132	-8.66E-06	-60.0304	0.178803
2734.34	0.000134	-7.43E-06	-48.0257	0.180723
2735.5	0.000135	-5.88E-06	-36.0188	0.1808
2708.17	0.000136	-4.07E-06	-24.0133	0.178993
2651.47	0.000137	-2.08E-06	-12.0067	0.175246
2566.58	0.000137	0	0	0.169635
2451.71	0.000137	2.08E-06	12.00667	0.162043
2306.12	0.000136	4.07E-06	24.01325	0.15242
2133.15	0.000135	5.88E-06	36.01882	0.140988
1944.85	0.000134	7.43E-06	48.02566	0.128543
1749.92	0.000132	8.66E-06	60.03042	0.115659
1562.29	0.00013	9.51E-06	72.03745	0.103258
1396.74	0.000128	9.95E-06	84.04423	0.092316
1259.33	0.000126	9.95E-06	96.04707	0.083234
1156.92	0.000124	9.51E-06	108.0538	0.076465
1088.42	0.000122	8.66E-06	120.0609	0.071938
1056.05	0.00012	7.43E-06	132.0656	0.069798
1059.78	0.000119	5.88E-06	144.0725	0.070045
1098.77	0.000118	4.07E-06	156.078	0.072622
1173.88	0.000117	2.08E-06	168.0846	0.077586
1285.09	0.000117	3.22E-21	180.0913	0.084937

Table –6: Nu for various angles over 3rd wire in 9-wire analyses at Re=0.015

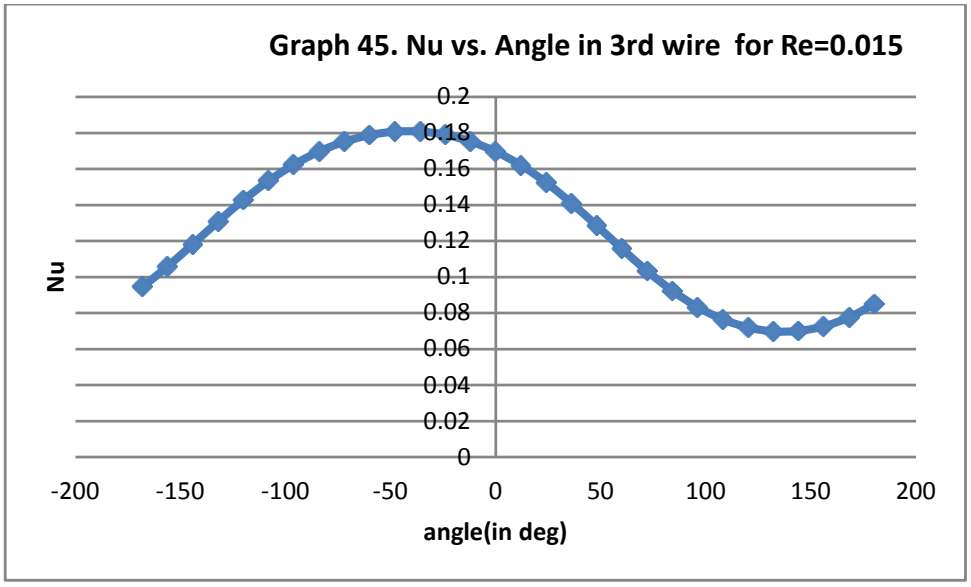
Graph 45. Nu vs. Angle in 3rd wire for Re=0.015
Nu
0.2
0.18
0.16
0.14
0.12
0.1
0.08
0.06
0.04
0.02
0
-200
-150
-100
-50
0
50
100
150
200
angle(in deg)

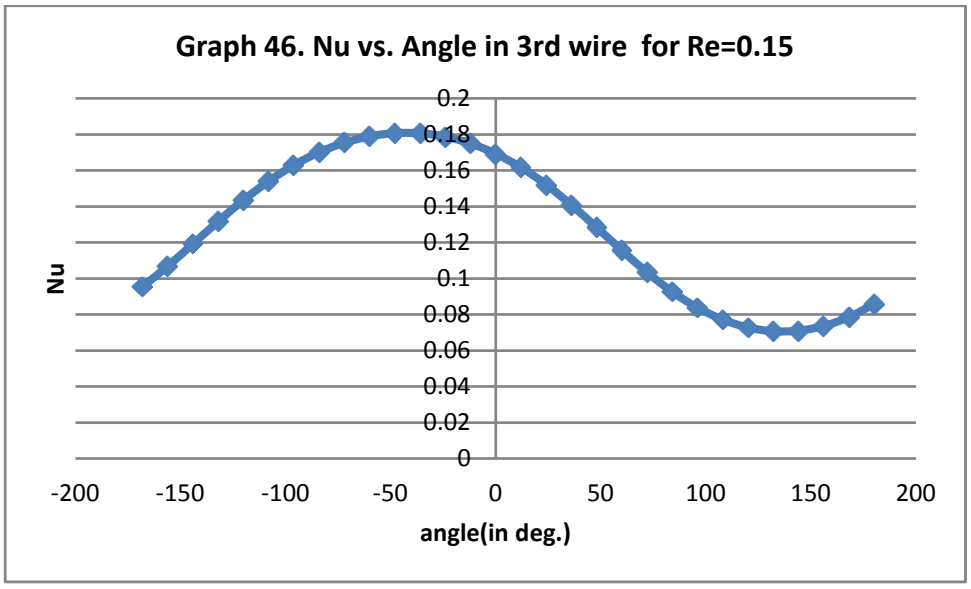
Graph 46. Nu vs. Angle in 3rd wire for Re=0.15
Nu
0.2
0.18
0.16
0.14
0.12
0.1
0.08
0.06
0.04
0.02
0
-200
-150
-100
-50
0
50
100
150
200
angle(in deg.)

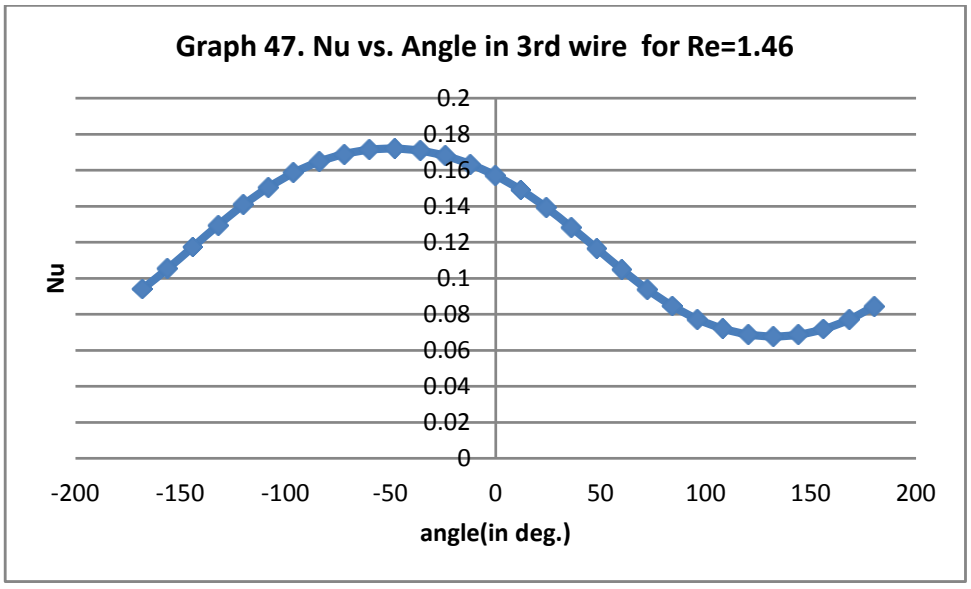
Graph 47. Nu vs. Angle in 3rd wire for Re=1.46
Nu
0.2
0.18
0.16
0.14
0.12
0.1
0.08
0.06
0.04
0.02
0
-200
-150
-100
-50
0
50
100
150
200
angle(in deg.)

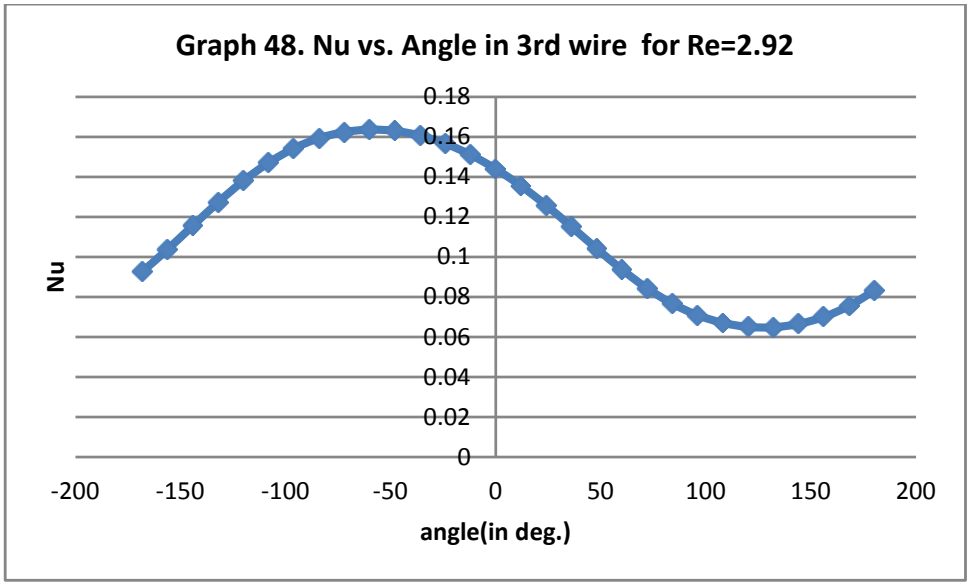
Graph 48. Nu vs. Angle in 3rd wire for Re=2.92
Nu
0.18
0.16
0.14
0.12
0.1
0.08
0.06
0.04
0.02
0
-200
-150
-100
-50
0
50
100
150
200
angle(in deg.)

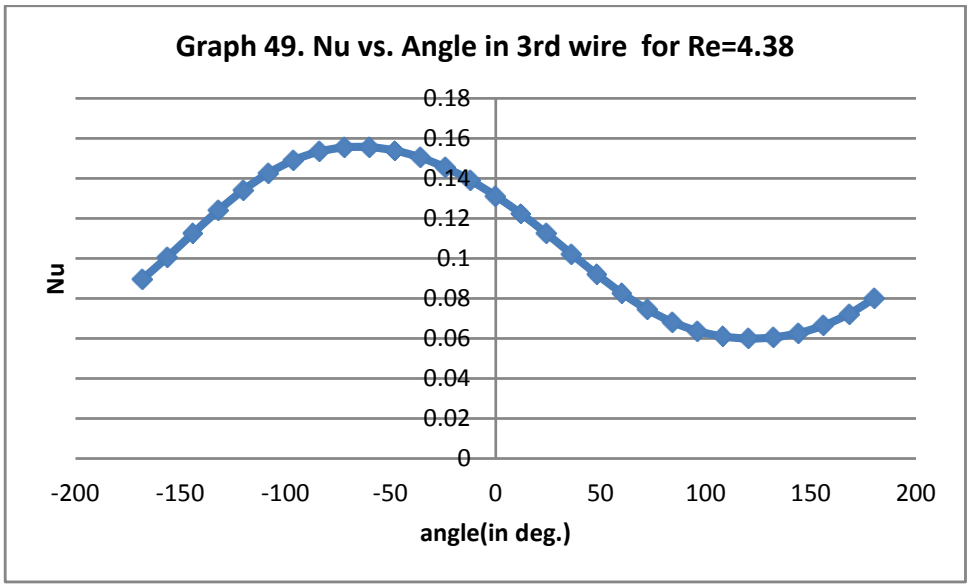
Graph 49. Nu vs. Angle in 3rd wire for Re=4.38
Nu
0.18
0.16
0.14
0.12
0.1
0.08
0.06
0.04
0.02
0
-200
-150
-100
-50
0
50
100
150
200
angle(in deg.)

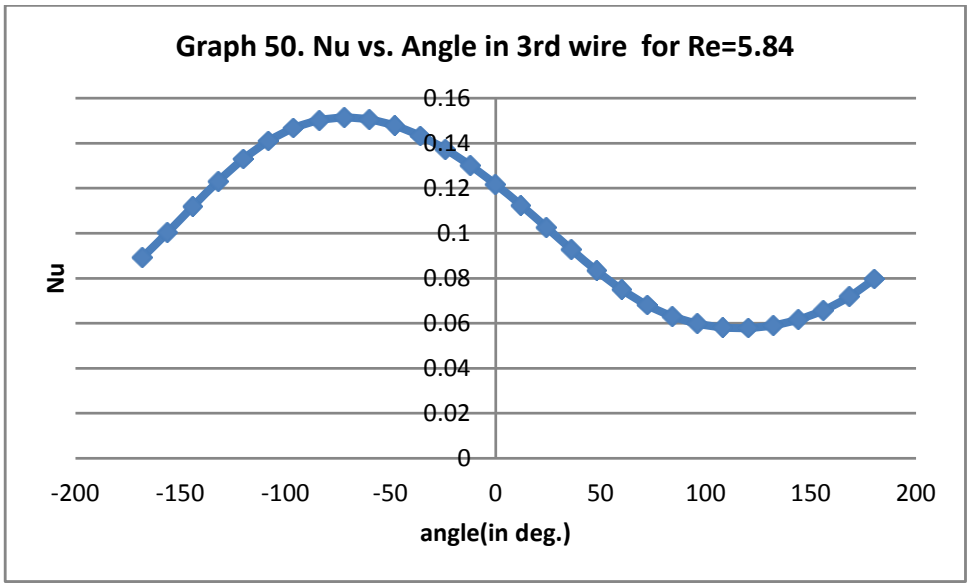
Graph 50. Nu vs. Angle in 3rd wire for Re=5.84
Nu
0.16
0.14
0.12
0.1
0.08
0.06
0.04
0.02
0
-200
-150
-100
-50
0
50
100
150
200
angle(in deg.)

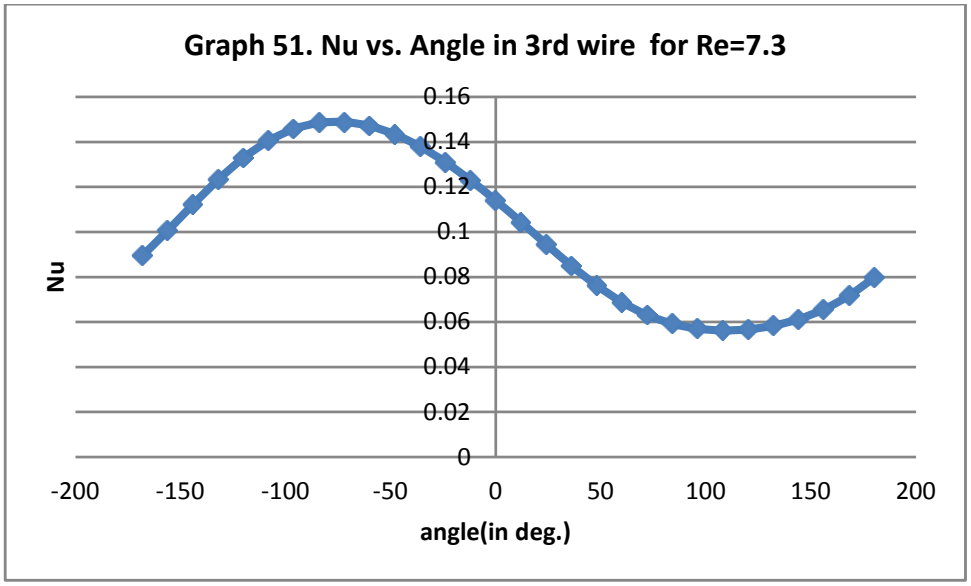
Graph 51. Nu vs. Angle in 3rd wire for Re=7.3
Nu
0.16
0.14
0.12
0.1
0.08
0.06
0.04
0.02
0
-200
-150
-100
-50
0
50
100
150
200
angle(in deg.)

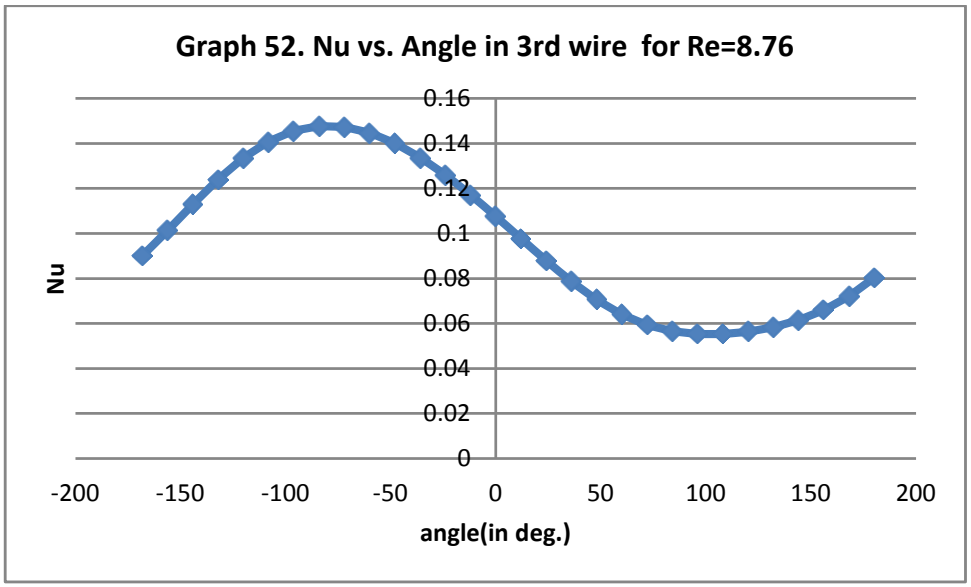
Graph 52. Nu vs. Angle in 3rd wire for Re=8.76
Nu
0.16
0.14
0.12
0.1
0.08
0.06
0.04
0.02
0
-200
-150
-100
-50
0
50
100
150
200
angle(in deg.)

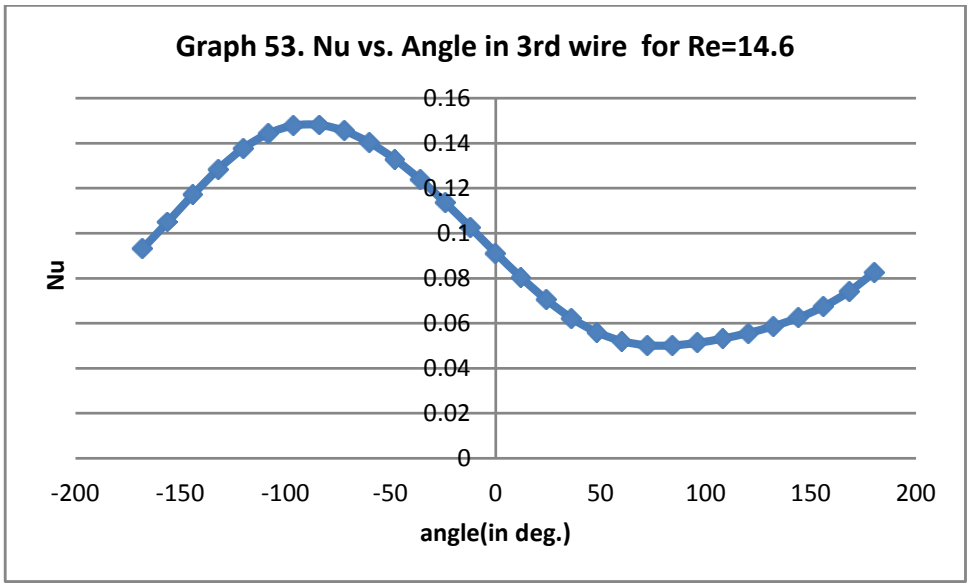
Graph 53. Nu vs. Angle in 3rd wire for Re=14.6
Nu
0.16
0.14
0.12
0.1
0.08
0.06
0.04
0.02
0
-200
-150
-100
-50
0
50
100
150
200
angle(in deg.)

The graphs are all similar with a slow shift to the left. The value of maximum and minimum Nu for higher Re is decreasing. This is quite different from the 2nd cylinder where the values remain almost unaffected by change in Re for the given range (0.015-15).The values of angle for minimum Nu vs. Re shows the following decreasing trend with increase in Re.

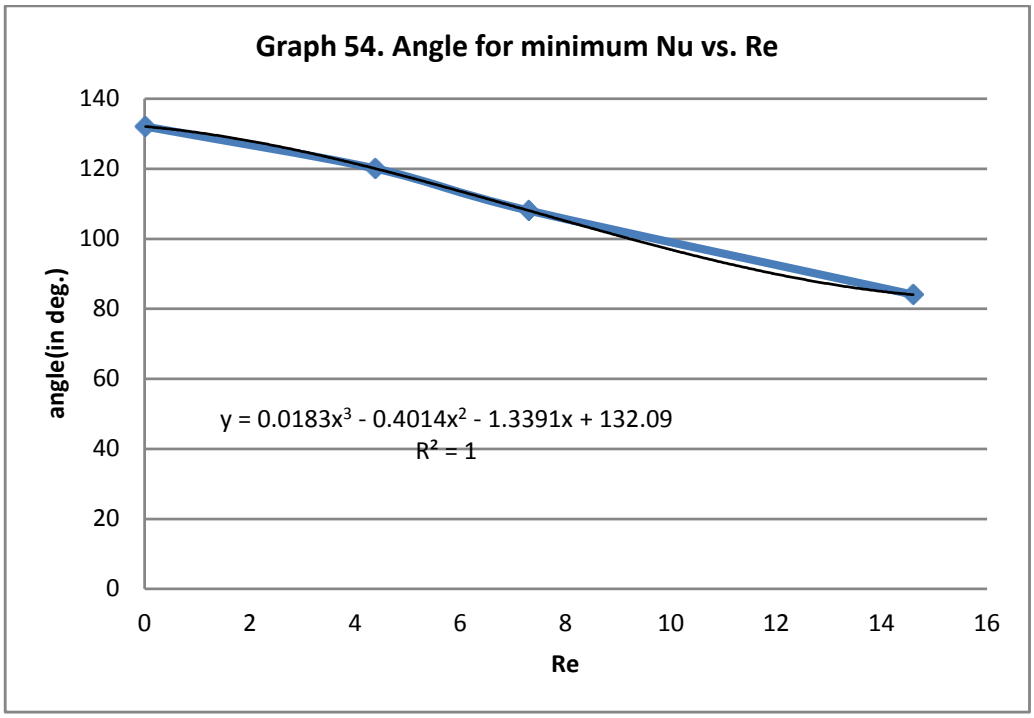

CHAPTER 8

WIRE MESH SCREEN ANALYSIS

Final wire mesh is now necessary for complete understanding of the flow. A wire mesh unlike a general wire analysis needs 3-D analysis as it has wires both horizontally and vertically.

The geometry for a 400 mesh is shown below with periodic and symmetry boundary condition used and modeling was done in FLUENT .This capability of fluent help to model the large symmetrical figure in very compact manner .Simplified geometry of wire mesh was taken as suggested by jhen [1], this will change little porosity and therefore deviation is small and hence simplified figure is accepted

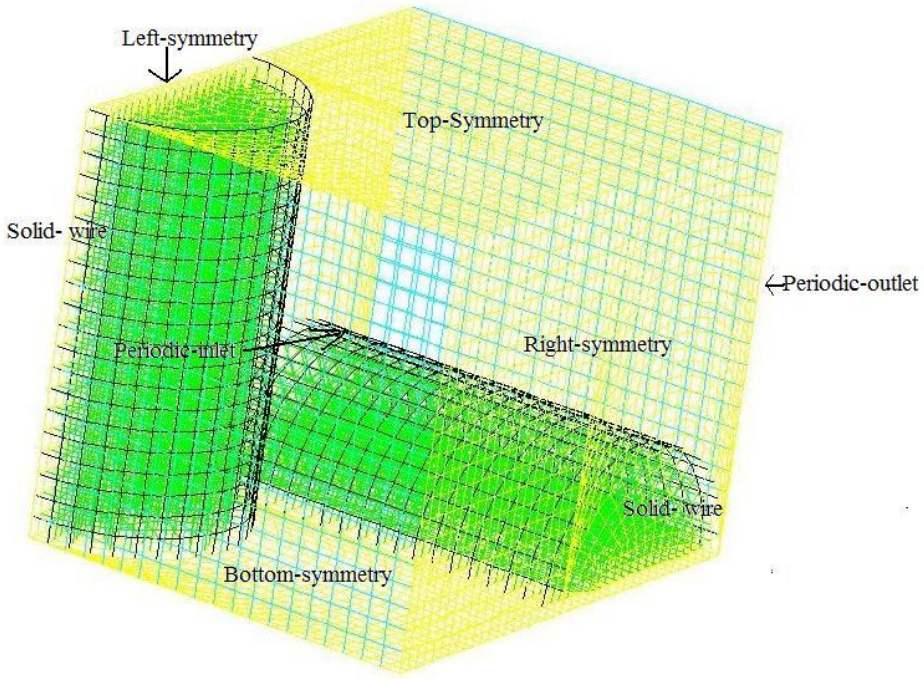

Fig .17 Mesh 3D-geometry

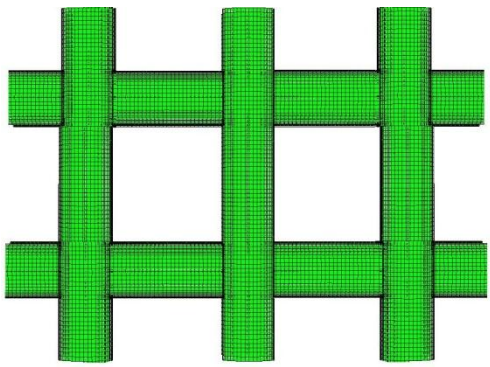

Fig.18 Geometry obtained by periodic repeat

Here the pitch (p) was taken to be $63.5X10^{-6}$ m. The diameter of the wire (D) was taken as $20X10^{-6}$ m. Pitch in both horizontal and vertical directions is same.

The graphs of pressure drop vs. Re shows a linear variation. The pressure drop increases with increase in Re.

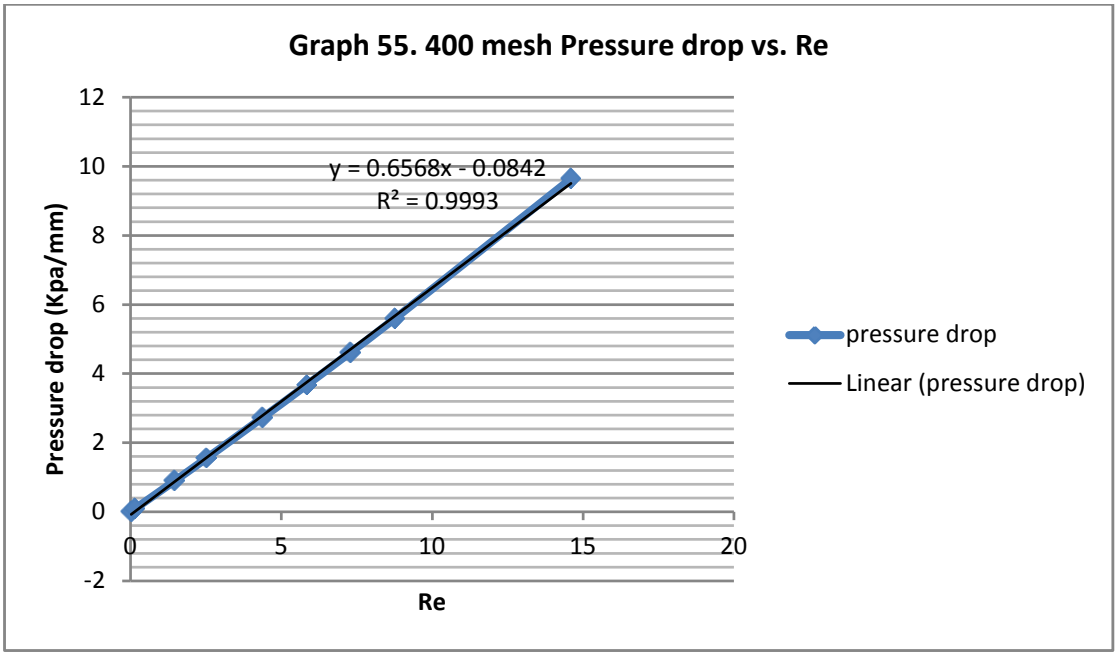

CONCLUSION

For single wire, the graphs show that the variation in Nu vs. angle is high for extremely low values of Re. But the value of average Nu increases with Re. The graph becomes flat as the value of Re approaches 1. Then it again ebbs more with increase in Re.

For 4 wires, the wires at the front had a similar flow pattern throughout with very little change in the point of minimum Nu. The shift was slowly towards angle (θ) $=0^{o}$. The variation is sinusoidal. For 2^{nd} wire, For low values of Re, the point of minimum Nu was at the upper part of the cylinder ($\theta=132^{o}$ for Re=0.015). As Re increased, the point shifted to back of the cylinder.

For 9 wires, the wire at the front for 2^{nd} row had a similar flow pattern throughout with very little change in the point of minimum Nu with gradual increase in the maximum and the minimum values. The graph seems to rise with increase in Re. In middle wire, the values of Nu at maxima and minima are almost same in all the graphs. The minima is slowly shifting towards $\theta=0^{0}$. In 3^{rd} wire, the graphs are all similar with a slow shift to the left. The value of maximum and minimum Nu for higher Re is decreasing. This is quite different from the 2nd cylinder where the values remain almost unaffected by change in Re for the given range (0.015-15).

Preesure drop along flow direction was plotted by changing velocity or Re .This graph is very useful for calculating pressure drop along any size of regenerator for particular Re.Suppose, Length of regenerator = 50mm.Pressure drop across regenerator (for Re = 1.46) = 0.8949*50 Kpa =44.75 Kpa

REFERENCES:

[1] Xu J.,Tian J.,Lu T.J,Hodson H.P.,On the thermal performance of wire- screen meshes asheat exchanger material. Int. J.Heat Mass Transfer 50 (2007) 1141-1154

[2] Binnun uri,Manitakos, Low cost high performance screen laminate regenerator matrix,Cryogenics 44 (2004) 439-444

[3] Versteeg H. K., Malalasekera W.,An introduction to Computational Fluid Dynamics,,Longman Scientific & technical ,Harlow, England

[4] S.Ergun,Fluid flow through packed columns,Chem.Eng. Prog.48 (1952) 89-94

[5] J.c.Armour,J.N. Cannon, Fluid flow through woven screens,AIChE J. 14 (1968) 415-421

[6] P.j.richards , M. Robinson,wind loads on porous structure , J.Wind Eng. Ind.Aerodyn. 83 (1999) 455 -465

[7] J.Tian,K.Kim,T.J Lu,H.P.Hodson,D.T. Queheillant,D.J.sypeck,H.N>G Wadley, The effects of topology upon fluid-flow and heat transfer within cellular copper structure ,Int. J. Heat Mass Transfer 47 (2004) 3171-3186.